Geomorphology 452 (2024) 109113

Contents lists available at ScienceDirect

Geomorphology

journal homepage: www.journals.elsevier.com/geomorphology

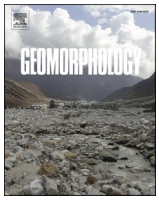

Deglaciation patterns in the Upper Zemmgrund, Austria: An exploration of clean-ice disintegration scenarios

H. Wytiahlowsky [a,*], M.E. Busfield [b], A.J. Hepburn [c], S. Lukas [d]

[a] Department of Geography, Durham University, Durham DH1 3LE, UK
[b] Department of Geography and Earth Sciences, Aberystwyth University, Aberystwyth SY23 3DB, UK
[c] European Space Astronomy Centre, European Space Agency, Madrid E-28692, Spain
[d] Department of Geology, University of Lund, Sölvegatan 12, 22362 Lund, Sweden

ARTICLE INFO

Keywords:
Paraglacial transition
Glacial geomorphology
European Alps
Glacier disintegration
Glacial change

ABSTRACT

The European Alps are rapidly losing glacier mass due to climatic warming and are anticipated to be largely ice-free by the year 2100. Long-term glacier monitoring in the Alps provides a record of anthropogenically-driven climate change since the Little Ice Age maximum in ~1850. Understanding these long-term glacier changes provides a basis for mitigating hazards (e.g., mass movements) associated with a transition to a paraglacial environment and for predicting future scenarios. Here, we present a post-Little Ice Age-maximum record of glacial landscape changes in the Upper Zemmgrund, Austria, utilising a multi-method framework integrating multi-decadal geomorphological mapping, historical imagery and remote sensing of glacier change. This study contributes a high-resolution, quantifiable record of the transition from a glacial to paraglacial landscape. We find that individual glacier response to climatic change varies within the Upper Zemmgrund, attributed to glacier characteristics such as hypsometry and size. Nonetheless, all glaciers show signs of growing instability such as an increase in crevasses and the collapse of circular tension structures, which have dammed meltwater at the terminus of one glacier, posing a substantial hazard to downstream communities. Future glacier disintegration is anticipated to accelerate in the Upper Zemmgrund, which may result in an ice-free landscape within the next ~40–60 years.

1. Introduction

Globally, contemporary glaciers are losing mass at the highest rate since observations began (Zemp et al., 2015, 2019). Glaciers and ice caps are losing mass at a faster rate than ice sheets, and whilst the largest glacier mass change rates have occurred in the Arctic, glacier mass loss is most directly felt in alpine regions, where glaciers have the highest rates of annual surface lowering and act as vital water towers for downstream communities (Zemp et al., 2019; Sommer et al., 2020; Hugonnet et al., 2021). High-mountain glaciers are sensitive indicators of climate change and provide freshwater for 10 % of the global population (Hock et al., 2019). Many high-alpine glaciated regions (e.g., the European Alps, North Caucasus and the tropical Andes) have already passed their peak water stage (Rets et al., 2020) and are experiencing reduced glacier runoff as a result. Under a modelled RCP 8.5 (high-emission) scenario (0.3 °C yr^{-1} temperature increase), these small glaciers are anticipated to lose >80 % of their mass by 2100 (Hock et al., 2019; Rounce et al., 2023), with the European Alps of particular concern as they are anticipated to be largely ice free (Zekollari et al., 2019). Glacier loss will be accompanied by both increased precipitation and more frequent, intense and prolonged droughts, which will increase the risk of associated hazards such as debris flows and flooding (Zemp et al., 2006; Gobiet et al., 2014; Žebre et al., 2021).

Long-term glacier monitoring offers a detailed archive of the impact of climatic warming. In the European Alps, such monitoring records the transition from the termination of the colder Little Ice Age (LIA) in 1850 (Grove and Switsur, 1994) to anomalously warm temperatures in the late 20th and early 21st centuries (Luterbacher et al., 2016). For example, Europe experienced summer air temperature warming of 1.3 °C between 1986 and 2015, which is greater than any period in the last 2000 years (Luterbacher et al., 2016). Previous studies have established a regional chronology of glacier change in the European Alps from radiocarbon dating, historical monitoring, and airborne/spaceborne imagery (e.g., Lambrecht and Kuhn, 2007; Pindur and Heuberger, 2008;

* Corresponding author.
E-mail address: holly.e.wytiahlowsky@durham.ac.uk (H. Wytiahlowsky).

https://doi.org/10.1016/j.geomorph.2024.109113
Received 27 October 2023; Received in revised form 15 February 2024; Accepted 21 February 2024
Available online 24 February 2024

Zemp et al., 2008; Zumbühl et al., 2008), revealing a pattern of net retreat, interrupted by small advances around 1890, 1920 and 1980. Understanding long-term glacier and landscape change provides a basis for predicting future scenarios and landscape evolution in populated alpine regions.

Effective glacier and landscape change monitoring and prediction requires an understanding of these changes at both regional and local scales. A detailed understanding of local glacial histories is particularly important for hazard mitigation (e.g., Williams et al., 2022) as previous hazard events (e.g., proglacial lake drainage events and/or rock slope failures) identify vulnerabilities within a landscape. Historical imagery has been integral for visualising long-term glacier changes in other regions of the European Alps and, when combined with local geomorphology and climatic records, can be used to understand past glacier dynamics at a high spatiotemporal resolution (e.g., Nussbaumer and Zumbühl, 2012; Zumbühl and Nussbaumer, 2018). Similar multi-method approaches have been undertaken more widely in the Arctic and its periphery (e.g., Hannesdóttir et al., 2015; Marlin et al., 2017; Ewertowski et al., 2019), providing an opportunity for the comparison of deglaciation scenarios under differing climatic boundary conditions.

Local geomorphological records can fill more recent gaps in regional glacier observation, such as the notable absence of glacier observation in the European Alps in the 1980s (Citterio et al., 2007). Local heterogeneity is also difficult to account for in regional projections of glacier mass loss, whether due to data availability or the computational expense associated with their inclusion in higher order models of ice flow (see Jouvet, 2023). Instead, studies may rely on sub-grid statistical parameterisations of variables known to be spatially heterogeneous (e.g., Fiddes and Gruber, 2014). Detailed observations at these scales are important to capture the influence of local factors (e.g., steep topography and highly variable climate) on glacier retreat, which in turn may better inform modelling studies.

Here, we combine observational and historical data to examine the ~170-year history of change within three neighbouring glacierised valleys in the Upper Zemmgrund, Austria. The Zemmgrund glaciers (2.7–3.4 km^2; 2015–16) exceed the mean Austrian glacier area (mean: 1.1 km^2, max: 16.1 km^2; 2015–16), however glaciers within the 1–5 km^2 class cover the largest combined area in the Alps (Paul et al., 2020) and the Zemmgrund was identified as a study site based on the proximity of accessible glaciers with differing characteristics. For example, Schwarzensteinkees' elevation range is typical of mean Austrian conditions, whereas Hornkees extends ~500 m below the mean minimum elevation of Austrian glaciers, and Waxeggkees extends ~250 m above the mean maximum elevation of Austrian glaciers. Therefore, the Zemmgrund glaciers provide a model for observing the different evolution of alpine glaciers with different hypsometries, and represent an ideal study locality in which to develop this approach due to Austria's regular glacier inventories (e.g., Patzelt, 1980; Fischer et al., 2015; Groß and Patzelt, 2015; Kuhn et al., 2015; Patzelt, 2015; Buckel and Otto, 2018), high-resolution orthophoto coverage, and extensive historical archives. Glacier retreat since the LIA maximum continues to expose a valuable geomorphological record, and here we demonstrate the utility of combining geomorphological, satellite and historical data to produce a high-resolution history of Alpine glacier dynamics throughout deglaciation. Glacier surface features (e.g., debris cover, crevasses) are influential in modulating ice melt and as such are integrated as a core component of our long-term record of glacier and landscape change (sensu Ballantyne, 2002; Glasser et al., 2016; Azzoni et al., 2017). A better understanding of the long-term rates and processes of post-LIA deglaciation is important if we are to measure the past and present impact of climate warming on vulnerable high-mountain areas, to understand both local and regional variability in climate response, and to be able to refine predictions on the future longevity of the mountain cryosphere. Therefore, the aim of this study is to map and quantify multi-decadal changes in proglacial geomorphology, glacier area, supraglacial debris cover and glacier structure, and evaluate intra-catchment variation in the response to climate warming, providing a framework with which to inform predictions on the future state of this and other similar catchments.

2. Study area

The Upper Zemmgrund Valley, Austria, contains three glaciers of contrasting geometries within the same catchment: Schwarzensteinkees, Waxeggkees, and Hornkees (Fig. 1). In 1850, the glaciers covered a total area of 18.3 km^2, but by 2015 this had been reduced to 8.31 km^2 (Buckel and Otto, 2018). Each glacier is north-orientated, situated in a cool, moderate climatic zone, and receives northern orographic precipitation, predominantly in summer (Pindur and Luzian, 2007; Pindur and Heuberger, 2008). Glacier elevation ranges from ~3100 metres above sea level (m.a.s.l) at the headwall to ~2400 m.a.s.l at Hornkees' terminus, with the surrounding ridges—including Großer Möseler—reaching a maximum elevation of 3480 m.a.s.l (Pindur and Luzian, 2007). The average equilibrium line altitude (ELA) for the three glaciers was 2630 m.a.s.l in 1850, rising 120–130 m in elevation by 1980 (Pindur and Heuberger, 2008). Glacier meltwater streams converge into the Zemmbach River and are diverted via a tunnel to the Schlegeis reservoir, which is used for hydropower generation.

The glacier forelands are dominated by sediment emplaced during an ice advance at 550 ± 70 cal. yr. BP, followed by two advances at ~400 and 300 cal. yr. BP (Mahaney et al., 2011). During the Holocene, seven dated advances are recorded within the stratigraphic and geomorphological record at Waxeggkees, ten at Hornkees and two at Schwarzensteinkees (Pindur and Heuberger, 2008). Earlier research in the Upper Zemmgrund establishes chronological control for moraine formation of ~1850 at the LIA maximum, ~1890, ~1920 and ~1980 (Humlum, 1978; Mahaney et al., 2011; Pindur and Heuberger, 2008; Wyshnytzky, 2017; Wyshnytzky et al., 2020). This study is the first to combine a full suite of multi-decadal satellite imagery, field geomorphology, and historical imagery to produce a quantifiable ~170-year record of glacier and landscape change through the glacial to paraglacial transition in the Upper Zemmgrund.

3. Methods

3.1. Data acquisition

We used satellite images, orthophotos, digital elevation models (DEMs), and historical imagery to map and quantify changes in the post-LIA glacier area, glacier surface features, and foreland geomorphology. Where possible, cloud-free imagery was acquired between July–September every ~3–5 years when snow cover is at a minimum to minimise the risk of recording annual fluctuations rather than long-term change (Table 1). High-resolution orthophotos (20 cm/pixel) were acquired from the State of Tirol for 1971, 2003, and 2019. All 1971 scenes are in greyscale, which may have restricted landform identification during geomorphological mapping. Two scenes for 2021 (9/10/21 and 30/10/21, the only scenes with <20 % cloud cover) were obtained from the European Space Agency Sentinel 2a satellite (10 m/pixel). One scene in 2005 (20/7/05) was obtained from the Advanced Spaceborne Thermal Emission and Reflection Radiometer (ASTER). A Google Earth 2015 base map was used to delineate 2015 glacier area, with the precise ground pixel resolution estimated to be between 1 and 5 m. We incorporated glacier outlines from the Austrian Glacier Inventory in 1969, 1999, 2011, and 2015 to supplement our measurements of glacier area change (Fischer et al., 2015; Groß and Patzelt, 2015; Kuhn et al., 2015; Patzelt, 2015). Additionally, five scenes were obtained from Planet SuperDove (3 m/pixel) to show the evolution of a collapse structure on Hornkees terminus between 2020 and 2022.

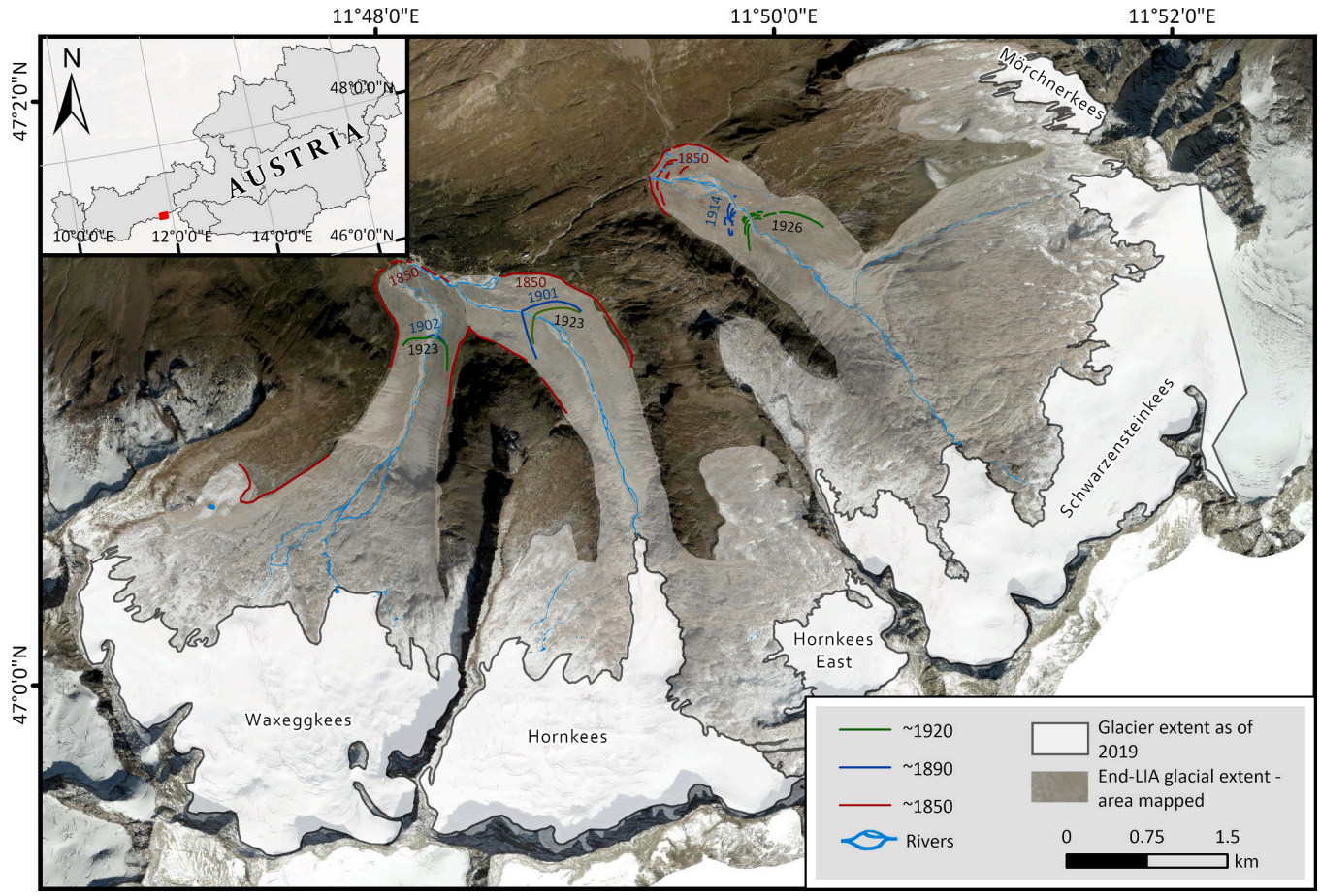

Fig. 1. The location of the Upper Zemmgrund glaciers, shown within the context of Austria. Glacier positions as of 2019 are shown in white and their forelands are demarcated by the 1850 frontal moraines.

3.2. Geomorphological mapping

Landforms and glacier surface features interpreted to be moraines, flutes, boulders, scree deposits, crevasses, and surficial debris cover were mapped from georeferenced 20 cm/pixel resolution orthophotos, using *ArcGIS Pro*. This was of a sufficiently high resolution to map features larger than 1 m. We limited our mapping of the foreland to within the LIA 1850 glacier extent shapefiles produced by Groß and Patzelt (2015). Following the framework for best practice outlined by Chandler et al. (2018) and Smith et al. (2006), a thematic mapping approach was taken to reduce cluttering. Vector layers delineating geomorphological features were created in an MGI Austria West local projection. Not all landforms are visible in every orthophoto due to differences in imaging conditions (e.g., shadowing). For example, flutes are visible in Schwarzensteinkees mid-foreland in 1971 and 2019 but cannot be seen in 2003 due to specific lighting conditions. Glacial grooves were mapped as polylines along a discernible centreline, all other features were mapped and digitised in polygon form based on their aerial footprint. We used hillshaded DEMs (~1 m resolution, 315° azimuth, 45° zenith) from Land Tirol (www.tirol.gv.at) to measure the height and length of landforms and to validate the positioning of features. The use of a single fixed hillshade may result in partial landform occlusion, however, interpretation bias is reduced by our use of multiple sources such as orthophotos and historical imagery. Fieldwork at the study site was undertaken annually in boreal summer 2014–2016 to conduct sedimentological analyses of individual landforms, the results of which have been reported elsewhere (e.g., Lukas and Busfield, 2017; Wyshnytzky et al., 2021). Field observations and photographs were used to qualitatively assess the results of mapping from remotely sensed imagery and to facilitate comparison with historical photographs and paintings. Aerial interpretations of foreland geomorphology were validated during a further visit to the field site in mid-June 2022.

3.3. Glacier area change

Glacier extent was manually delineated from Sentinel 2, Google Earth, and Land Tirol imagery for 2003, 2005, 2015, 2019 and 2021. A sinusoidal Lambert Azimuthal Equal Area projection was used to calculate geometries. Surface area (km^2) was compared to the previous observation to calculate glacier area change, expressed as a percentage of the LIA maximum. Annual rates of glacier surface area change were calculated by dividing the difference in area between consecutive timestamps by the number of years between them. Errors in manual glacier delineation were estimated following DeBeer and Sharp (2007), who argue that line placement uncertainty is likely to be larger than the imagery resolution for clean glaciers with unobscured imagery coverage. Here, we assume the measurement error is equal to the polygon perimeter multiplied by pixel resolution. For example, in 2021, the perimeter of Schwarzensteinkees was digitised at 23,431 m from 10 m ground pixel resolution Sentinel-2a imagery, giving a measurement error of 2.94 ± 0.23 km^2.

3.4. Historical imagery

In the absence of high-resolution satellite imagery before 1971, historical field photos and maps were used to infer glacier area and landscape change. *Inkscape* (1.0) image editing software was used to annotate and compare historical and modern imagery. Where possible,

Table 1
The imagery and shapefile data used to delineate glacier area and for geomorphological mapping in the Upper Zemmgrund. The specific date of acquisition is not provided for Land Tirol orthophotos, although all orthophotos have minimal snow cover and are assumed to have been acquired during the summer period. * Indicates that a secondary scene was used to delineate glacier margins where minor cloud cover was present.

Satellite (platform)	Spatial resolution	Spectral bands	Dates*	Source
Aerial survey (LiDAR)	~0.5 m	N/A	1969	https://doi.org/10.1594/PANGAEA.844983
Aerial survey (orthophoto)	20 cm	N/A (greyscale)	1971	Land Tirol (maps.tirol.gv.at)
Aerial survey (LiDAR)	~0.5 m	N/A	1999	https://doi.org/10.1594/PANGAEA.844984
Aerial survey (orthophoto)	20 cm	N/A	2003	Land Tirol (maps.tirol.gv.at)
Terra	15 m	B1: (0.52–0.60 μm) B2: (0.63–0.69 μm) B3N: (0.78–0.86 μm)	20th July 2005	NASA (https://earthdata.nasa.gov/)
Aerial survey (orthophoto)	~0.5 m	N/A	2011	https://doi.org/10.1594/PANGAEA.844988
WorldView	~1–2 m	N/A	31st July 2015	Google Earth (earth.google.co.uk)
Aerial survey (orthophoto)	20 cm	N/A	2019	Land Tirol (maps.tirol.gv.at)
Sentinel-2A	10 m	B2: (490 μm) B3: (560 μm) B4: (665 μm)	10th* October 2021 (30th used where minor cloud cover)	USGS (earthexplorer.usgs.gov)
SuperDove	3 m	B2: (490 μm) B4: (565 μm) B6: (665 μm)	26th August 2020 19th August 2021 2nd July 2022 30th July 2022 11th November 2023	Planet Labs (planet.com)
Aerial survey (orthophoto)	20 cm	N/A	2022	Land Tirol (maps.tirol.gv.at)

imagery was obtained from the same perspective and bedrock markers were used as ground control points to estimate glacier area change. Historical imagery is most effective when incorporated as part of a multi-method approach (Williams et al., 2022) due to uncertainties in camera position/parameters and the lack of georeferencing therein.

4. Results

4.1. Proglacial landform change – LIA to 2019

4.1.1. Schwarzensteinkees

The forelands of Schwarzensteinkees and adjacent Mörchnerkees (Fig. 1) are delineated by frontal moraines formed during the ~1850 LIA maximum (Pindur and Heuberger, 2008), with hummocky terrain extending beyond the distal margin of the frontal moraines. The ~1850 moraines are boulder-strewn, 664 m in length, ~40–50 m wide, ~5 m high, and are breached in several locations by meltwater streams (Fig. 2b). Direct glacier observations are not available for the 1850s, but a painting by Ender (1841) depicts the Schwarzensteinkees proglacial landscape in close proximity to the ice front, characterised by areas of ice-moulded bedrock, similar to the modern foreland, onto which an elongate moraine has been deposited (Fig. 3a). The painting does not depict abundant supraglacial debris at the ice margin in the mid-19th century (Fig. 3a). The ice front is in contact with a small sediment ridge, with retreat from this position exposing the small (~6 m wide), closely-spaced moraines seen behind the ~1850 frontal moraine in the modern foreland (Fig. 3a–d); they are of reduced width and height compared to the ~1850 moraines (Fig. 3d). The area surrounding these small moraines is characterised by a higher concentration of boulders than more ice-proximal regions of the foreland (Fig. 2b).

To the south of the 1850 moraine complex, the terrain is flat with no depositional landforms and there is a general absence of boulders (Fig. 2b). Military surveys in 1807/08 depict a pro-glacial lake in this area, which ceased to exist as the glacier re-advanced towards the ~1850 moraines between 1869 and 1887 (Fig. 4).

Between the 1869 to 1887 military survey and the first satellite imagery in 1971, two sets of more low-lying moraines (<3 m high) were deposited within the foreland in close succession in ~1914 and ~1926 (Figs. 2, 4; Pindur and Heuberger, 2008). The ~1926 moraines show greater preservation, with a more sharply defined and foreland-wide arcuate shape. By 1971, the meltwater stream had dissected both moraine assemblages, with the ~1914 moraines observed primarily to the west of the stream (Fig. 2b). After 1926, no depositional landforms have been recorded southwards towards the 1971 ice margin (Fig. 2b). The availability of satellite imagery in 1971 allows for the documentation of higher elevation areas not visible from the ground perspective of historical photos, revealing large bedrock exposures infilled by sediment in the upper reaches (Fig. 2b).

Schwarzensteinkees advanced in line with the rest of the Zemmgrund glaciers between 1966 and 1980 (Fig. 3b & c). No landform deposition is evident from this advance at Schwarzensteinkees, and there appears to be minimal supraglacial debris cover at the proglacial margin in the 1971 orthophotos (Fig. 2b).

In imagery from 2003, a set of ice-marginal moraines is visible for the first time following the retreat of the western glacial lobe (Fig. 2d). In addition, the heavily crevassed regions at the glacier front collapsed exposing large areas of bedrock. The ~1914 and ~1926 moraines in the central parts of the foreland of Schwarzensteinkees show further fragmentation and erosion, with the width of both Mörchnerkees' and Schwarzensteinkees' lateral moraines also notably reduced due to downslope fluting of sediment (Fig. 2d). The maximum width of the braided meltwater streams had reduced from ~25 m wide in 1971 to ~12 m wide in 2003 and became confined to a smaller portion of the foreland, with evidence of channel abandonment further south (Fig. 2).

Between 2003 and 2019, the preservation of the Mörchnerkees frontal moraines and upper lateral moraines continued to decline (Fig. 2). The retreat of Mörchnerkees exposed large regions of unconsolidated sediment cover, in contrast to the large areas of ice-marginal bedrock with minimal unconsolidated sediment infill in front of Schwarzensteinkees (Fig. 2f). The width and number of active river channels remained in decline following a decrease in glacier area (Fig. 2). The width of active river channels reduced to ~2–10 m wide

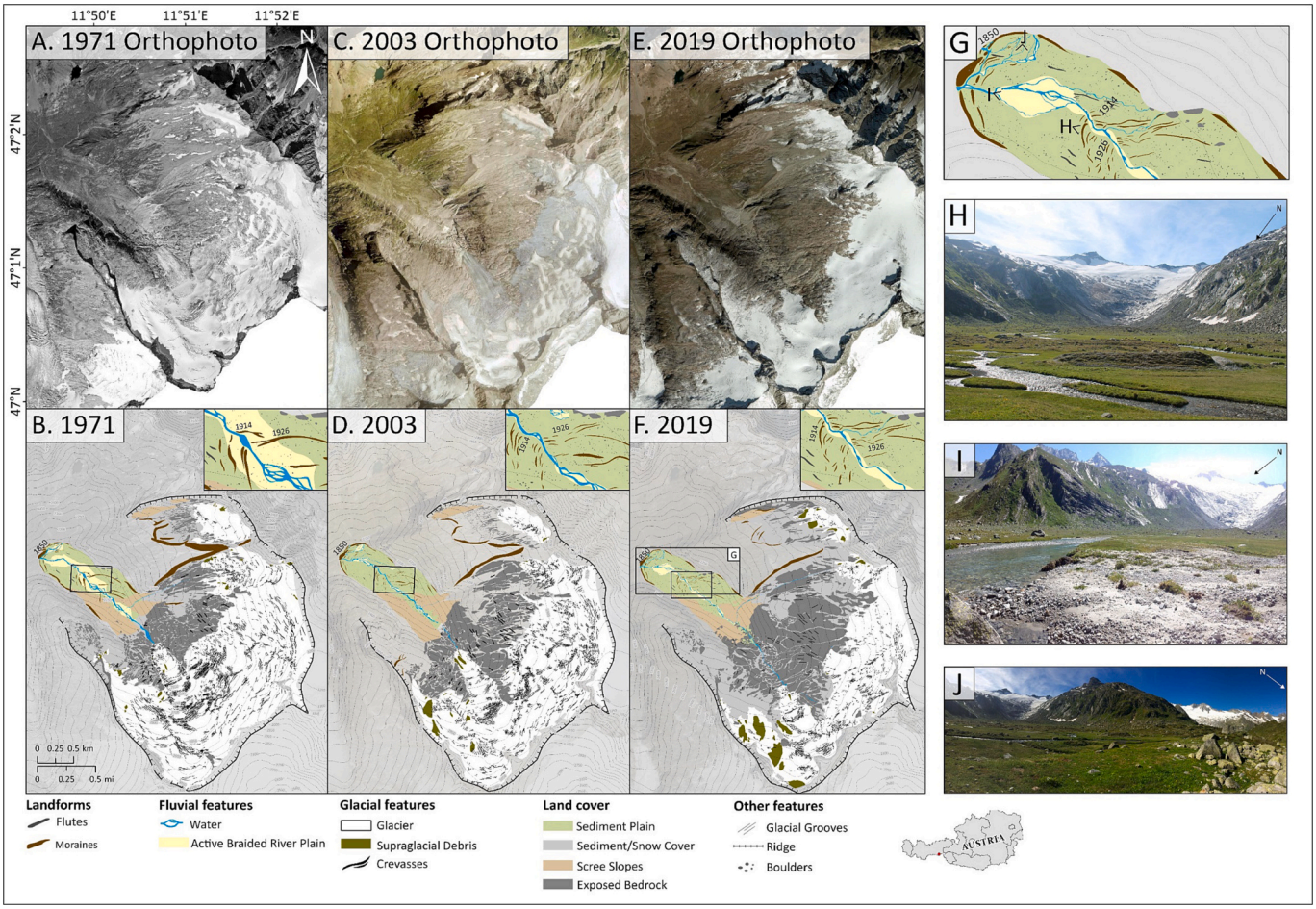

Fig. 2. Geomorphological maps of Schwarzensteinkees in 1971 (B), 2003 (D) and 2019 (F) produced from the corresponding orthophotos (above). The location and perspective of panels H–J are shown in panel G. (G) Schwarzensteinkees foreland, with the extent shown in panel F. (H) Looking south of the outermost moraines towards the ice margin in 2016. (I) Looking towards the moraines formed in ~1914 in 2015. (J) The outermost Schwarzensteinkees moraines looking west in 2016.

and river discharge became increasingly confined to one larger channel, with a reduction in braiding (Fig. 2).

4.1.2. Hornkees

Hornkees' foreland is delineated by a thin ~1850 frontal moraine (~6 m wide, ~2–3 m high) on its north-eastern margin, with an absence of moraines on the north-western foreland margin (Fig. 5b). Historical imagery shows that Hornkees and Waxeggkees converged at the north-western foreland margin; however, by 1879, Hornkees had retreated and was no longer confluent with Waxeggkees (Figs. 4, 6a). In 1879, Hornkees is in direct contact with the lateral moraines on its eastern margin (Fig. 6a). The ice margin is characterised by thin, longitudinal debris stripes, although debris cover is less extensive than at the current margin (Figs. 5, 6a). In front of the 1879 snout, a striated glacial pavement records former, pre-LIA, north-westerly flow towards Waxeggkees (Figs. 5, 6a).

Hornkees was in net recession after 1879 except for two advances dated to ~1901 and ~1923 (Fig. 5; Pindur and Heuberger, 2008). These advances are recorded by two moraines (~80 m apart), spanning most of the foreland width (Fig. 5). By 1966, Hornkees had retreated ~790 m south of the 1923 moraine (Figs. 5, 6b). Vegetation had begun to colonise the top and northernmost slopes of the lateral moraines and scree had progressively accumulated at their bases (Fig. 6b). Glacier recession led to the exposure of two broadly valley-parallel elongate landforms in the centre of the valley, adjacent to the main meltwater stream. The first is approximately 300 m south of the 1923 moraine and is partly dissected by meltwater streams on its western margin (Fig. 5b). The second is situated in front of the 1966 ice margin, distinguished as an elongate area of higher relief which had been incised by meltwater streams on both margins by 2008 (Fig. 6b & d).

In the 1980s, a minor re-advance of Hornkees is documented by a small moraine up-valley of the southernmost elongate landform (Fig. 5d). However, Hornkees is the only Zemmgrund glacier with a preserved geomorphological record of this advance. Debris cover at the glacier terminus reduced between 1966 and 1980, preceding the ~1980s glacial advance (Fig. 6b & c). The ice-contact slope of the southernmost elongate landform (exposed before 1966; seen in 6b–d) was overridden by the glacier in ~1980 and re-exposed following subsequent glacier retreat (Fig. 6c).

A thin (~8 m wide), arcuate moraine spanning approximately a third of the foreland width is visible by 2003, ~395 m south of the elongate landform first exposed running along the centre of the valley in the 1971 imagery (Fig. 5d). Between 2003 and 2019, the collapse of part of Hornkees' terminus exposes a small moraine ridge, south of the 1980s moraine (Fig. 5). The moraine crest is located at the 2003 ice margin and is of a similar width to the 1980s moraine. Between 1850 and 2019, the north-eastern ~1850 lateral moraines show an increase in width, whereas the moraines near the valley centre narrow and become more fragmented (Fig. 5).

4.1.3. Waxeggkees

A series of ~10 m wide and ~2 m high moraines (formed ~1850) mark the north-western limit of the Waxeggkees foreland. These moraines are dissected by meltwater streams (Fig. 7b). The absence of

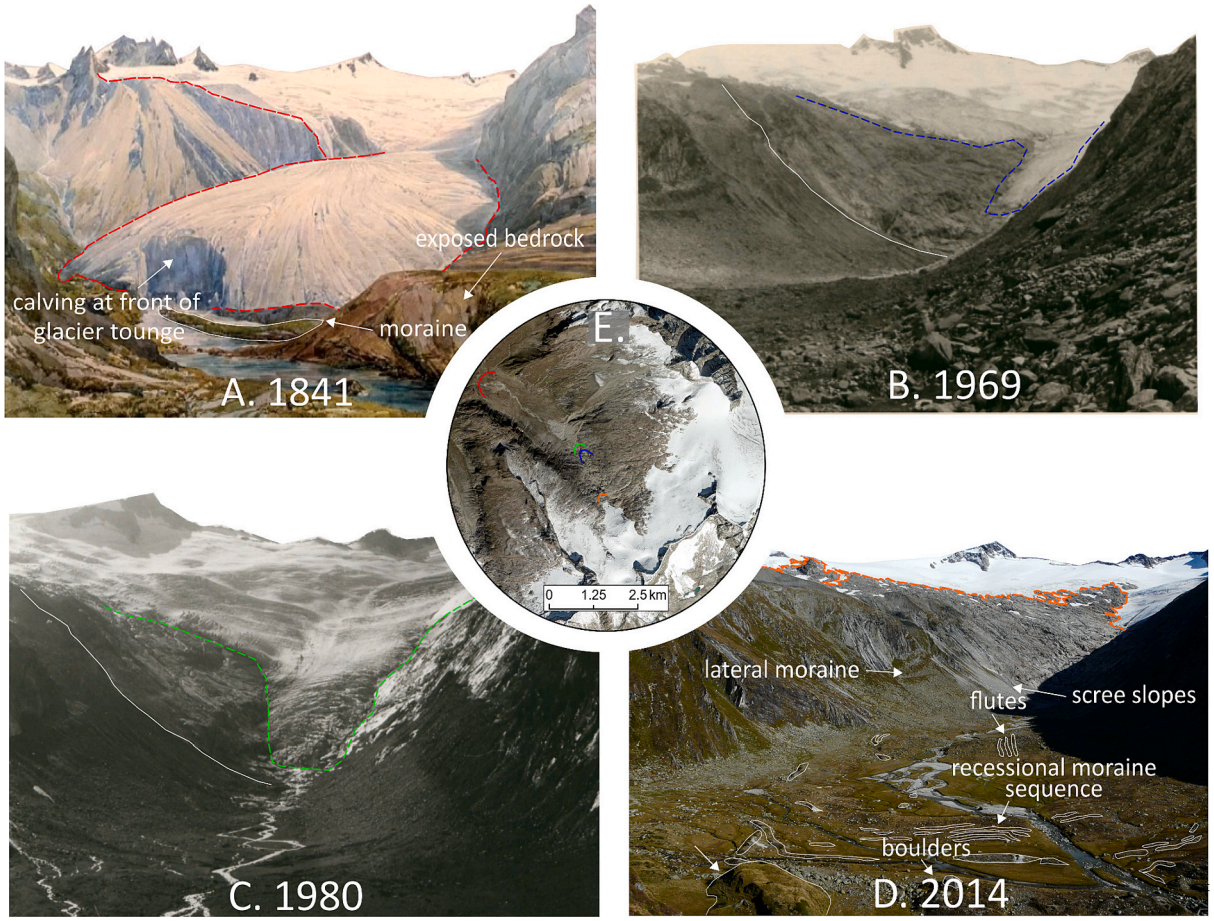

Fig. 3. Schwarzensteinkees glacial change. (a) Water colour painting of the Schwarzensteinkees foreland in ~1841 annotated with landforms (Ender, 1841) modified after 1841 as part of this study under the Creative Commons 3.0 license. (b) Schwarzensteinkees photographed in 1969. (c) Schwarzensteinkees glacier in photographed in 1980. (d) The Schwarzensteinkees foreland photographed in 2014. (e) A 2019 orthophoto depicting inferred changes in glacier terminus position. Line colour corresponds with the panel where the same colour is used to digitise glacier outlines.

~1850 frontal moraines on the north-eastern side of the valley is likely due to the confluence with Hornkees glacier in ~1850. The lateral moraines here are the most pronounced in the Zemmgrund with the lowest relief slope (32°), compared to 38° at both Hornkees and Schwarzensteinkees.

South of the frontal moraines at Waxeggkees, two episodes of glacier advance are documented by two arcuate moraines that span almost the entire width of the foreland (Fig. 7); these have been dated to ~1902 and ~1923 (Pindur and Heuberger, 2008). In imagery from 1901, the glacier front is obscured but the glacier terminus is seen to narrow downvalley and extends across less than half the width of the foreland (Fig. 8a). The ~1902 moraine has subsequently been dissected by meltwater streams, leaving only its eastern margin preserved (Fig. 7). The ~1923 moraine is better preserved, asymmetric, and protrudes further south on its eastern side (Fig. 7).

By 1950, Waxeggkees had retreated to a hanging glacier configuration, with a large bedrock ridge below the glacier terminus exposed for the first time (Fig. 8b). The distal end of the lateral moraines is no longer in contact with the glacier terminus and the eastern lateral moraine is notably steeper (Fig. 8b). By 1966, the lateral moraines of Waxeggkees had accumulated more scree at their base than observed at Schwarzensteinkees and Hornkees (Figs. 3b, 6b, 8c). Vegetation had begun to colonise the lower slopes of the northern (distal) ends of the lateral moraines but had not yet reached the moraine crests as seen at Hornkees in 1966 (Fig. 8c).

By 1971, the glacier terminus had retreated to above the bedrock ridge and was surrounded by areas of bedrock thinly covered by sediment (Fig. 7). Between 1966 and 1980, a minor advance of Waxeggkees is apparent, with the glacier extending ~200 m further down the bedrock ridge (Fig. 8c–d). No depositional evidence of this advance is recorded, nor was it sufficient for the glacier to extend down to the valley floor.

By 2000, the lateral moraines of Waxeggkees had become sharply defined and show a minor increase in the downslope transfer of sediment (Fig. 8e). By 2003, the ~1902 and ~1923 moraines became increasingly dissected and reduced in width (Fig. 7). Glacier retreat continued to expose more bedrock, although large areas of the ice-margin remain covered by unconsolidated sediment (Fig. 7).

Vegetation had mostly colonised the lateral moraines in 2015 except for the scree slopes immediately adjacent to the bedrock platform (Fig. 8f). Retreat between 2003 and 2019 primarily exposed unconsolidated sediment rather than bedrock, and surrounding bedrock has since become increasingly infilled by sediment (Fig. 7). The ~1902 moraine has been heavily eroded and is only well-preserved on its eastern side. Meltwater channel width declined from ~2–13 m in 2003 to ~2–6 m in 2019, accompanied by a reduction in the number of braided channels most notable in the northern (distal) end of the foreland (Fig. 7).

4.2. *Glacial & supraglacial change*

At the LIA maximum in 1850, Schwarzensteinkees covered 7.94 km^2, Hornkees covered 5.68 km^2, and Waxeggkees covered 5.05 km^2 (Table 2). Following this maximum, a general pattern of net retreat occurred, interrupted by two periods of advance, recorded by moraine

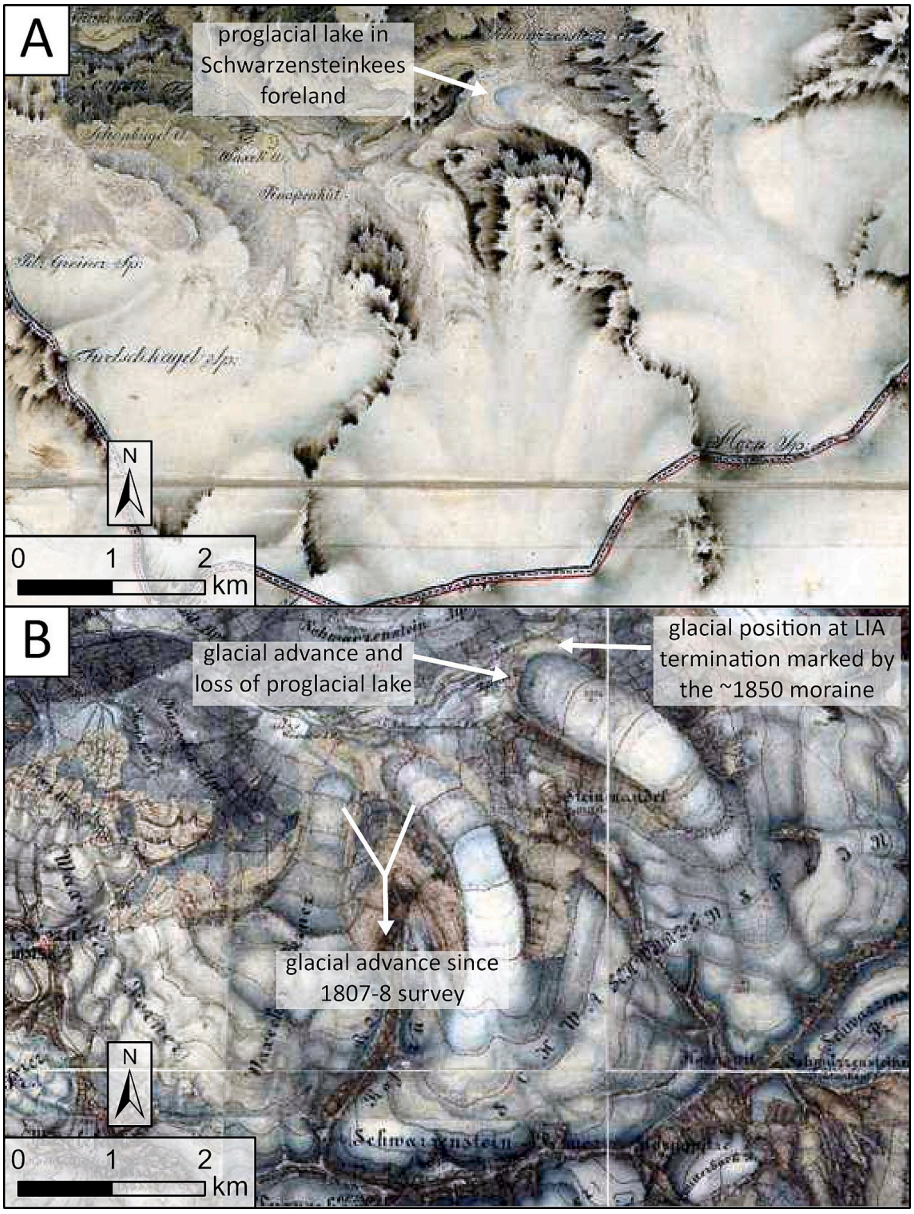

Fig. 4. Historical military survey maps of the Habsburg Empire. (a) The Upper Zemmgrund glaciers in the second military survey of the Habsburg Empire (1807–1808) (Timár et al., 2006). (b) The Upper Zemmgrund glaciers in the third military survey of the Habsburg Empire (1869–1887) (Timár et al., 2006).

formation in ~1890 and ~1920 (Fig. 9). In 1969, aerial surveys of glacier area provided the first quantifiable measure of glacier surface area, with Waxeggkees occupying the largest proportion of its LIA extent (77 %) (Table 2).

Between 1969 and 1999, the rate of surface area change (0.02 km^2 yr^{-1}) was the same for all glaciers (Table 2), however, this period was interrupted by an advance in the ~1980s (Figs. 9; 10). By 1999, optical imagery shows that thinning of Hornkees glacier has resulted in the formation of a new glacier, which has decoupled from the main glacier in the upper reaches (Fig. 9). Over a similar period (1971 to 2003), the crevassed area of all glaciers increased, with the highest rates of retreat corresponding with areas with a high density of crevasses (Table 3). Debris cover also slightly increased on all glaciers between 1971 and 2003. Where debris is present, scattered coverage is minimal, and all glaciers remain predominantly debris-free (Table 4).

Schwarzensteinkees and Waxeggkees underwent their fastest rate of retreat between 2011 and 2015 (−0.15 km^2 yr^{-1}), whereas for Hornkees this took place between 2015 and 2019 (−0.09 km^2 yr^{-1}) (Table 2). However, there is uncertainty as to whether retreat rates decreased in the early 2000s and between 2019 and 2021 due to the higher error margin resulting from coarser imagery (10 m resolution) (Tables 1, 2). A collapse of a heavily-crevassed and debris-covered part of Hornkees terminus occurred between 2015 and 2019, leaving behind a small peninsula extending from the glacier terminus (Fig. 5). This collapse resulted in a decrease in overall debris cover at Hornkees, with Waxeggkees and Schwarzensteinkees showing a slight decrease and increase in debris cover, respectively (Table 4). Between 2003 and 2019, crevasses per km^2 at Waxeggkees increased by 55 %, concentrated in the mid-reaches, 17 % at Hornkees, and 8 % at Schwarzensteinkees (Table 3). As of 2021, the Zemmgrund glaciers cover a combined area of 7.65 km^2, with Schwarzensteinkees remaining the largest glacier (2.94 km^2), followed by Waxeggkees (2.42 km^2) which is now larger than Hornkees (2.29 km^2) (Table 2; Fig. 10).

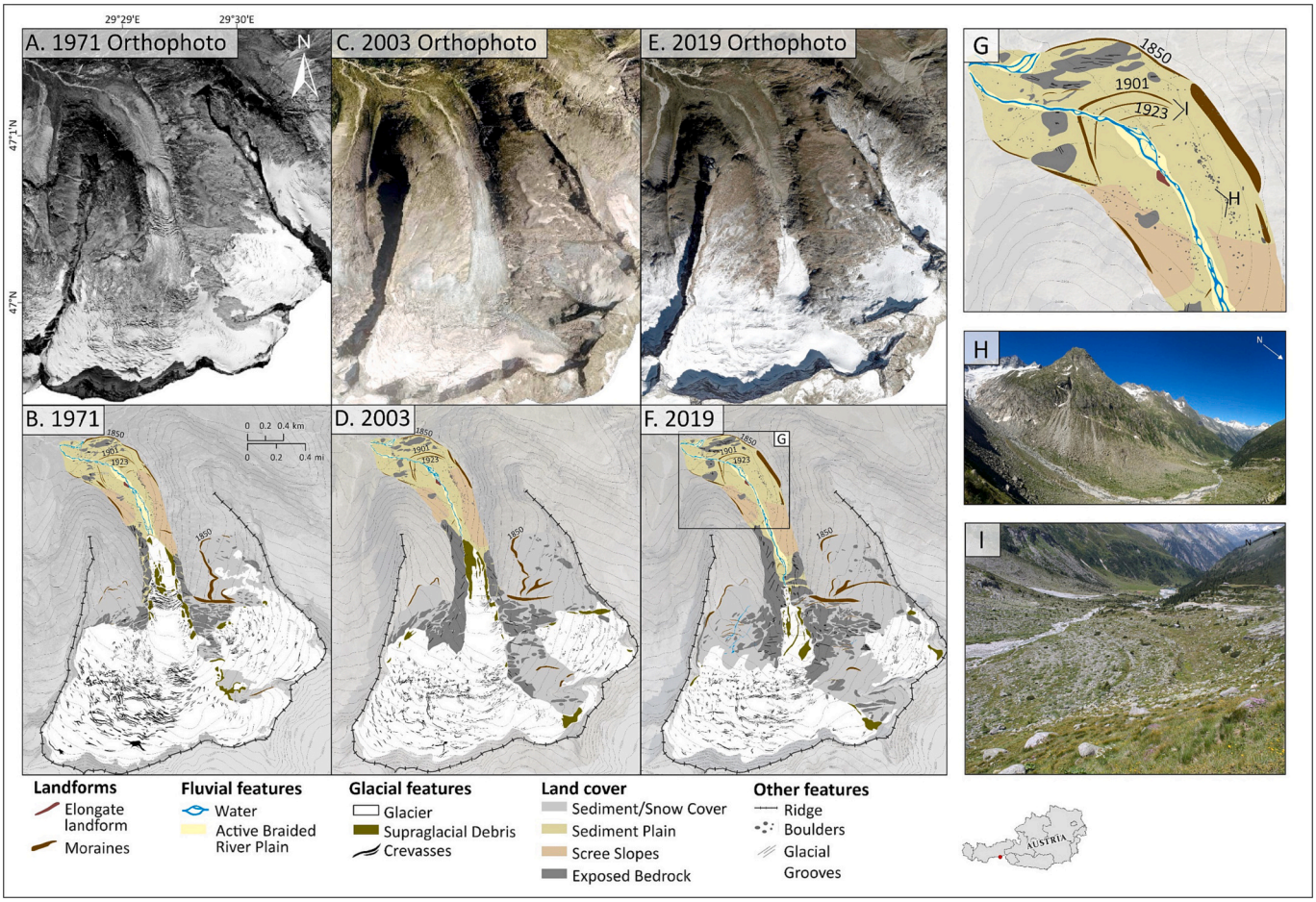

Fig. 5. Geomorphological maps of Hornkees glacier in 1971 (B), 2003 (D) and 2019 (F) produced from the corresponding orthophotos (above). The location and perspective of panels H–I are shown in panel G. (G) Hornkees foreland, with the extent shown in panel F. (H) Looking west towards Hornkees lateral moraines and mid-foreland in 2016. (I) Hornkees moraines in 2016 formed ~1901 and ~1923.

5. Discussion and interpretation

5.1. Geomorphological processes

In the Upper Zemmgrund, glacier extent at the Little Ice Age maximum is marked by large frontal moraines within each foreland, with formation constrained to ~1850 (Pindur and Heuberger, 2008; Figs. 2, 5, 7). However, no ~1850 frontal moraines are preserved at the eastern and western margins of Waxeggkees and Hornkees respectively, suggesting an adjoined ice surface at the LIA maximum. It is unlikely that this confluence was long-lived. Prior to the maximum in 1807/8 the glaciers were separate, with their ice margins situated close to the ~1890 moraine position (Figs. 4; 9). Photo documentation of Hornkees shows that the glaciers were no longer confluent by 1879 (Fig. 6a), supporting convergence within a ~40-year interval preceding the LIA maximum, and separation within <30 years thereafter. It is possible that retreat from the ~1850 maximum allowed for short-lived damming of meltwater in the Hornkees foreland, upvalley of Waxeggkees, but this is considered unlikely. Boulder-free, flat terrain in the Schwarzensteinkees foreland provides strong geomorphological and sedimentary evidence for the establishment of a lacustrine environment (Wyshnytzky, 2017; Wyshnytzky et al., 2020, 2021), whereas the foreland south of Hornkees' LIA maximum is still characterised by a high concentration of boulders (Figs. 2, 5). Instead, we suggest that meltwater from Hornkees was diverted north around Waxeggkees' snout to merge with the Zemmbach River, reflected in the current river organisation.

Retreat from the ~1850 maximum was interrupted by a period of cooling in the 1890s, which resulted in moraine formation at all glaciers in the Upper Zemmgrund (Fig. 9), consistent with 50 to 70 % of Austrian glaciers (Rott, 1993). Prior to this advance, Hornkees was mostly free of supraglacial debris except for a few bands which were orientated parallel to the valley long-axis and emerged at the glacier snout (Fig. 6a). As the moraine is almost continuous and there is no evidence of any rockfall events, the debris for moraine formation is likely predominantly subglacial in origin (Fig. 5). At Hornkees and Waxeggkees this advance is recorded by a singular arcuate moraine, albeit less pronounced at Waxeggkees (Figs. 5, 7). In Schwarzensteinkees' foreland, moraines are more closely spaced than at Waxeggkees and Hornkees, indicating significant fluctuations at the glacier front during the period of cooling (Fig. 2). Moraine formation at Schwarzensteinkees occurred ten years after Hornkees and Waxeggkees, with glacier retreat along a centreline occurring at a similar rate at all glaciers (12 to 13 m yr^{-1}, 1850–1980). This delay in moraine formation suggests that Schwarzensteinkees is slightly slower to respond to climatic perturbations than Hornkees and Waxeggkees (see Section 5.2.1).

By ~1920, a second period of moraine formation is recorded across all glaciers in the Zemmgrund (Fig. 9). Moraine formation is mostly synchronous, with the delay in moraine formation at Schwarzensteinkees reduced to three years, compared to a 10-year lag in response previously (Fig. 9). Waxeggkees' ~1920 moraine spans more than two thirds of the valley width (Fig. 7); its westward margin appears to have partly collapsed due to what we attribute to be the melt out of an ice cored moraine. The limited retreat from the ~1890 to ~1920 moraines of only 16 m indicates that Waxeggkees may have stagnated at this

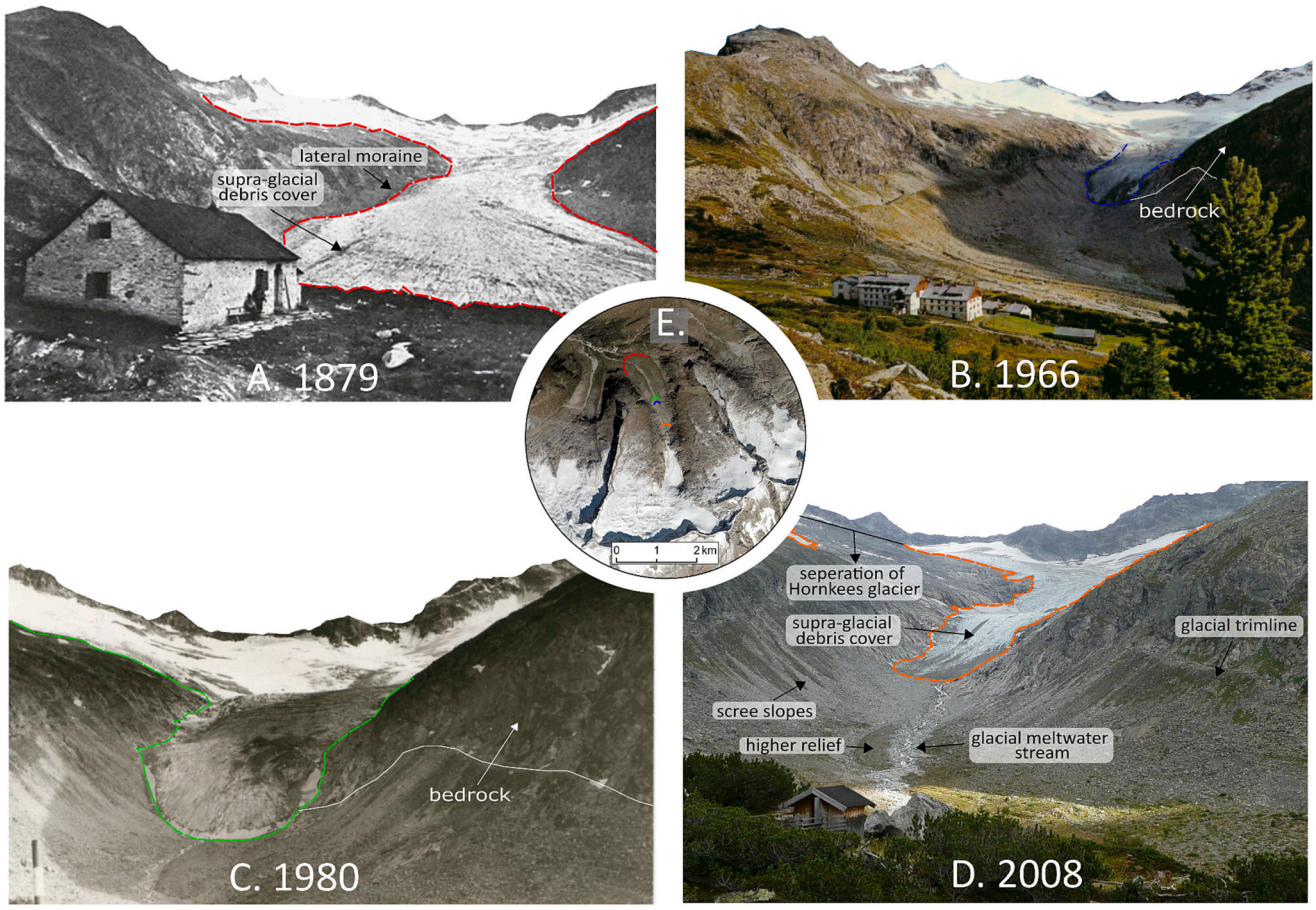

Fig. 6. Hornkees glacial change (a) Hornkees after to the 1850 LIA maximum (Johannes, 1919). (b) Hornkees photographed in 1966. (c) Hornkees glacier photographed advancing in 1980. (d) The view from Berliner Hütte looking towards Hornkees in 2008 (e) A 2019 orthophoto depicting inferred changes in glacier terminus position. Line colour corresponds with the panel where the same colour is used to digitise glacier outlines.

margin during this period, whereas Hornkees and Schwarzensteinkees retreated by 91 and 113 m, respectively. Hornkees is the only glacier to have two clear arcuate ~1890 and ~1920 moraines that are continuous, aside from one breach of each moraine by meltwater streams at the centre of the valley (Fig. 5). Compared to the ~1890 moraine, the ~1920 moraine is narrower and is ~15 m lower in altitude, inferring a reduction in sediment supply at the snout and thinning of the glacier surface between advances (Fig. 5).

Geomorphological evidence of a ~1980s advance is recorded solely within the Hornkees foreland (Figs. 5; 9). Moraine formation in a high-alpine setting at a temperate glacier margin typically occurs by a combination of dumping and ice-push (Benn and Evans, 2010; Lukas and Sass, 2011; Lukas et al., 2012; Lukas, 2012; Rettig et al., 2023). Mapping from 1971 imagery shows that Hornkees is the only glacier with adequate sediment supply at the ice margin and with a thicker sediment sequence overlying the bedrock. Thus, it is possible that pushing and dumping mechanisms contributed to the formation of the 1980s Hornkees moraine. An absence of imagery and direct glacier observations in the 1980s means we cannot confirm moraines were not formed at Schwarzensteinkees and Waxeggkees and later subjected to post-depositional modification and removal. However, as no further advances are recorded post-1980s, and Hornkees' 1980 moraine remains preserved, it is likely that limited sediment supply may have precluded their formation.

Following this final advance, glaciers in the Zemmgrund have undergone an uninterrupted pattern of net retreat, with landscape and geomorphological change now predominantly a result of non-glacial processes. Despite increased glacier melt, the reduction in glacier area has resulted in an overall reduction in seasonal meltwater discharge evident from a decline in braided channels and overall channel width (Figs. 2, 5, 7). The glaciofluvial influence has become confined to a smaller proportion of the foreland, with increased vegetation colonisation of the riverbanks and on the lateral moraines, aiding stability and reducing downslope fluting of sediment. The lateral moraines remain the best-preserved features over our observational period, despite some evidence of gullying on their proximal sides. They have undergone minimal alteration in their height and appearance since orthophoto surveys began (1971) as the forelands were already predominantly deglaciated and the moraine slopes have since increased in stability. This is in accordance with observations at other Alpine glaciers, which show that lateral moraines have high preservation potential, with the highest erosion rates corresponding with recently deglaciated slopes facing the glacier (Eichel et al., 2018). However, higher rates of alteration have been recorded in some examples where slopes are subject either to greater landslide activity, the combined action of sliding, debris fall and debris flow processes, and/or the melt-out of dead ice masses (e.g., Curry et al., 2006; Lukas et al., 2012; Dusik et al., 2019; Betz-Nutz et al., 2023). In the Upper Zemmgrund, small moraines exhibit the poorest preservation within the mid-forelands, notably for the low amplitude, closely-spaced moraines that are present within Schwarzensteinkees' foreland, which show a visible reduction in size over an observational period of four years (Wyshnytzky, 2017). This decline in active glacial modification of the landscape marks a transition towards paraglacial relaxation and eventually ice-free Alps.

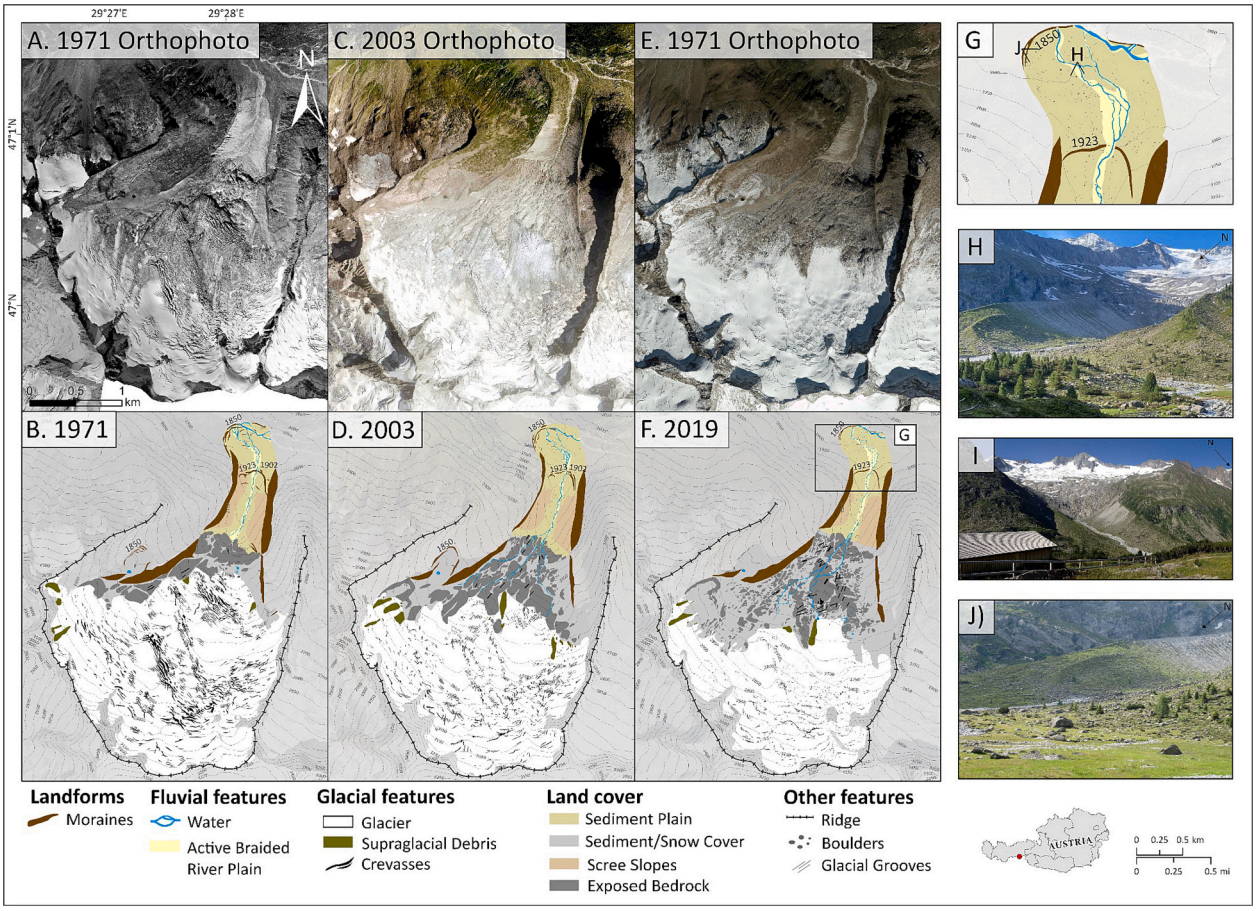

Fig. 7. Geomorphological maps of Waxeggkees glacier in 1971 (B), 2003 (D) and 2019 (F) produced from the corresponding orthophotos (above). The location and perspective of panels H–J are shown in panel G. (G) the northern margins of Waxeggkees foreland, with the extent shown in panel F. (H) Looking southeast towards Waxeggkees formed ~1923 moraine in 2022. (I) Waxeggkees glacier and lateral moraines in 2016. (J) Waxeggkees eastern lateral moraine and foreland in 2016.

5.2. Glacial processes

5.2.1. Drivers of glacier retreat

Whilst the overall retreat rates of the Upper Zemmgrund glaciers are broadly consistent with glaciers of the same size class within Austria (1–5 km^2, 1969–2005: Abermann et al., 2009), there is a large disparity in the time-lag between moraine formation and retreat rates amongst the Zemmgrund glaciers. This is most evident from the 10-year delay in moraine formation in response to climate forcing in the ~1890s at Schwarzensteinkees compared to Waxeggkees and Hornkees. By the 1920s, the time-lag in moraine formation at Schwarzensteinkees had reduced to ~3-years behind Hornkees and Waxeggkees, with the glacier now exhibiting a faster response to changes in mass balance (Figs. 2, 5, 7). As all glaciers have similar aspects and climatic conditions, we attribute the delay in moraine formation to differential glacier characteristics, notably size, in this case as Schwarzensteinkees was >1 km^2 larger (~23 % larger in 1969) than the other glaciers. This observation is in accordance with Pfeffer et al. (1998) who note that smaller glaciers often respond faster to climatic perturbations as they often possess steeper surface slopes. Interestingly, however, several studies also note that though larger glaciers may respond to shifts in mass balance more slowly, they tend to lose more area overall (e.g., Jiskoot et al., 2009; Paul and Mölg, 2014). The Upper Zemmgrund glaciers reinforce the role of glacier size as a predictor of area loss, with the largest surface area in 1850 corresponding with the highest rates of area change, and vice versa.

The effect of hypsometry on glacier retreat is also clearly exhibited within the Upper Zemmgrund by the change in configuration of Waxeggkees' area-elevation distribution. At the LIA maximum, all glaciers were situated on the valley floor, with each glacier's frontal moraines at the following elevations: Schwarzensteinkees at 2100 m, Hornkees at 1920 m and Waxeggkees at 1880 m. In ~1850, all glaciers exhibited a valley glacier configuration, with the larger glaciers situated at higher elevations, however by 1950 Waxeggkees had transitioned into a hanging glacier, now situated in a bedrock bowl above the valley floor (Fig. 8b). In contrast, Hornkees still extended down valley to a much lower altitude. By 2021, Hornkees had shrunk to 40 % of its LIA maximum area and is now smaller than Waxeggkees which retained 48 % of its LIA area, despite Hornkees formerly exceeding Waxeggkees in size by >0.5 km^2 at the LIA maximum (Table 2). We attribute this difference in retreat to glacier hypsometry, as Hornkees retained a larger proportion of its mass in the ablation area below the ELA (~2850 m, 2022), whereas most of Waxeggkees is situated at higher elevations with a smaller ablation area (Žebre et al., 2021). Similarly, numerous studies (e.g., Kuhn et al., 1985; De Angelis, 2014; Gharehchahi et al., 2021) have also attributed a bottom-heavy area-elevation distribution and the presence of ice at lower elevations to increased melt rates, faster retreat, and increased sensitivity to climate change. This highlights the vulnerability of larger glaciers extending to lower elevations compared to small, often topographically shaded, cirques that exist at higher elevations. These larger glaciers are particularly vulnerable to disconnections (i.e., thinning over ice falls) and a lack of snow replenishment in the ablation area. Hence, in order to constrain accurate predictions of glacier longevity, it is important that large-scale modelling of climatic forcing accounts for variations in glacier hypsometry and corresponding response times.

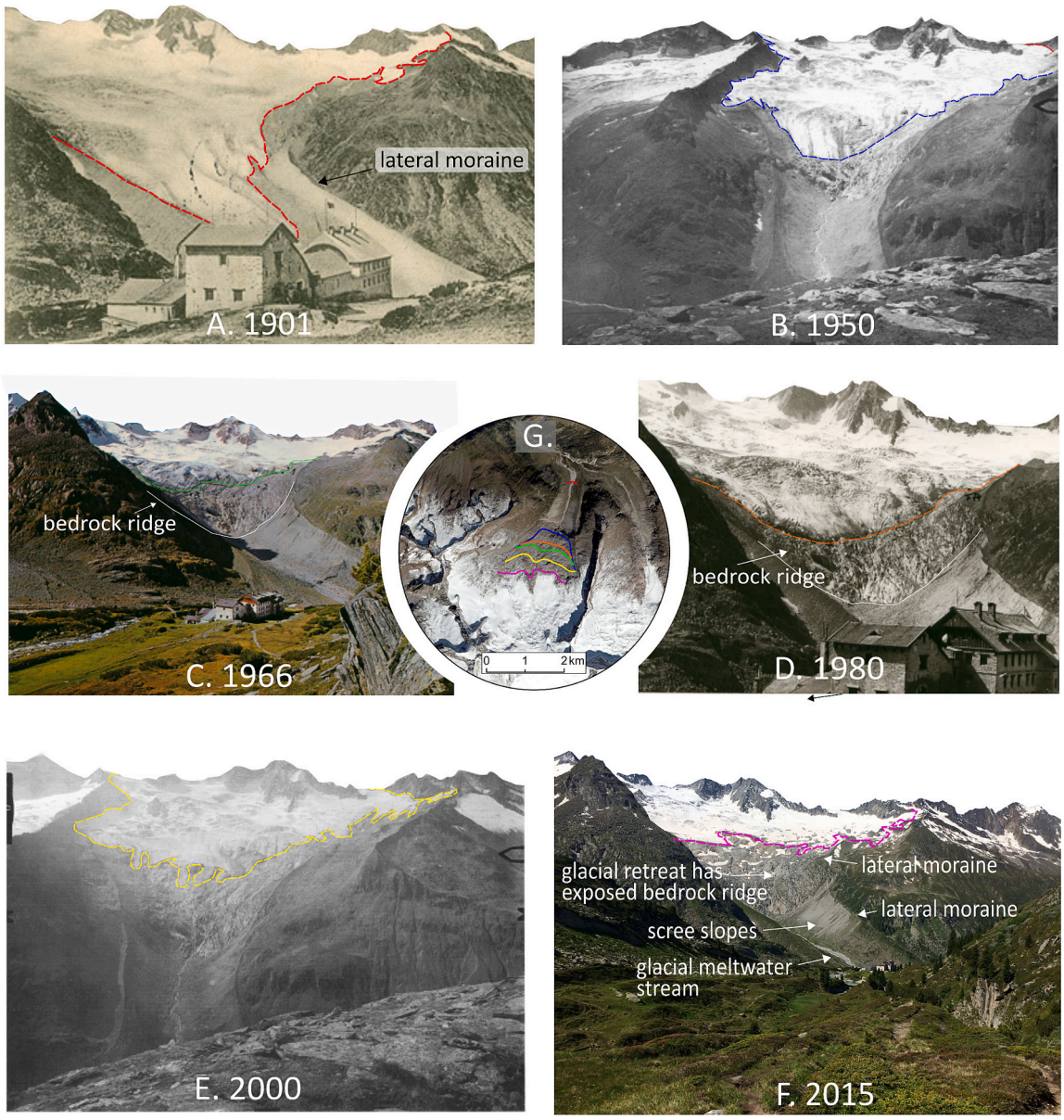

Fig. 8. Waxeggkees glacial change. (a) A postcard showing Waxeggkees glacier as seen from Berliner Hütte in 1901. (b) Waxeggkees glacier in 1950 (Brunner and Rentsch, 2002). (c) Waxeggkees glacier photographed in 1966. (d) Waxeggkees glacier photographed in 1980. (e) Waxeggkees glacier in 2000 (Brunner and Rentsch, 2002). (f) Waxeggkees glacial foreland photographed in 2015. (g) A 2019 orthophoto depicting inferred changes in glacier terminus position. Line colour corresponds with the panel where the same colour is used to digitise glacier outlines.

5.2.2. Debris cover

All glaciers have undergone a minor increase in debris cover since the 1970s, but remain mostly 'clean', with debris cover peaking in the early 2000s (Table 4). The increase in debris cover in the early 2000s may potentially be attributed to the 2003 heatwave, which Keiler et al. (2010) note led to an increase in wind-blown dust being deposited on glaciers in the European Alps leading to a lower surface albedo. However, the primary source of supraglacial debris is likely a combination of downwasting across the glacier surface leading to the exposure of englacial debris and some rockfall events that have been transported along flowlines (e.g., Goodsell et al., 2005; Lukas et al., 2005). This is supported by the concentration of debris at the glacier termini, with debris gradually emerging at the surface through melt-out rather than being passively transported supraglacially along a substantial portion of the glacier. No major rockfall events have been recorded in the Zemmgrund. However, debris below the headwall at the eastern margins of Schwarzensteinkees and Waxeggkees has increased from 1971 to 2019 (Figs. 2, 7). This is attributed to increased thawing of permafrost and glacier ice, likely reducing the stability of the surrounding mountain ridge. Depending on the thickness of the debris cover, this increase in debris has the potential to either accelerate (reduced albedo) or decelerate (increased insulation) the rate of glacier retreat (Juen et al., 2014; Glasser et al., 2016; Fleischer et al., 2021). It is possible that debris cover on Hornkees accelerated the collapse of part of its terminus between 2003 and 2019. However, it is difficult to disentangle the relative contribution of climatic warming and a reduced surface albedo.

Here, we argue that notable insulation or accelerated ablation due to debris cover is unlikely. In the Eastern European Alps, the impact of debris cover on melt rates and mass balance is subdued compared to other high mountain regions (Fleischer et al., 2021). Retreat rates of glaciers with varying debris cover were shown to be primarily controlled by rising temperatures which outweighed the rate at which debris accumulated (Fleischer et al., 2021). Modelling scenarios in the European Alps have shown that a 10 % debris cover with a thickness of 6 cm

Table 2
Changes in glacier surface area from 1850 to 2021 at Schwarzensteinkees, Hornkees and Waxeggkees glaciers. Dates with an asterisk next to them indicate that data for these dates were obtained from the Austrian Glacier Inventories. Error margins are specified for each year mapped.

Year	Area (km^2)	Area change (km^2)	Area change (km^2 yr^{-1})	% Change from previous area	Ice cover change since LIA (LIA = 100 %)
			Schwarzensteinkees Glacier (including Mörchnerkees)		
2021 (±0.23)	2.94	−0.10	−0.05	−3.29 %	37.03
2019 (±0.005)	3.04	−0.31	−0.08	−9.25 %	38.29
2015 (±0.005)	3.35	−0.59	−0.15	−14.97 %	42.19
2011*	3.94	−0.11	−0.02	−2.72 %	49.62
2005 (±0.28)	4.05	−0.04	−0.02	−0.98 %	51.01
2003 (±0.004)	4.09	−0.28	−0.07	−6.41 %	51.51
1999*	4.37	−0.63	−0.02	−12.60 %	55.04
1969*	5.00	−2.94	−0.02	−37.03 %	62.97
LIA*	7.94				100.00
			Hornkees Glacier		
2021 (±0.15)	2.29	−0.06	−0.03	−2.55 %	40.32
2019 (±0.003)	2.35	−0.37	−0.09	−13.60 %	41.37
2015 (±0.003)	2.72	−0.23	−0.06	−7.80 %	47.89
2011*	2.95	−0.14	−0.02	−4.53 %	51.94
2005 (±0.24)	3.09	0.07	0.03	2.32 %	54.40
2003 (±0.003)	3.02	−0.26	−0.06	−7.93 %	53.17
1999*	3.28	−0.69	−0.02	−17.38 %	57.75
1969*	3.97	−1.71	−0.01	−30.11 %	69.89
LIA*	5.68				100.00
			Waxeggkees Glacier		
2021 (±0.14)	2.42	−0.05	−0.03	−2.02 %	47.92
2019 (±0.002)	2.47	−0.17	−0.04	−6.44 %	48.91
2015 (±0.02)	2.64	−0.60	−0.15	−18.52 %	52.28
2011*	3.24	0.10	0.02	3.18 %	64.16
2005 (±0.19)	3.14	−0.10	−0.05	−3.09 %	62.18
2003 (±0.002)	3.24	−0.10	−0.02	−2.99 %	64.16
1999*	3.34	−0.56	−0.02	−14.36 %	66.14
1969*	3.9	−1.15	−0.01	−22.77 %	77.23
LIA*	5.05				100.00

can reduce surface runoff by 7 % (Reid et al., 2012). However, we deem a drastic increase in supraglacial debris to be unlikely in the Upper Zemmgrund because debris cover mostly consists of a discontinuous scattering of small pebbles and boulders, rather than continuous blankets of thick sediment. This scattering is confined to lower elevations, with most of the ice at higher elevations remaining completely debris free. This may be attributed to the topography of the Upper Zemmgrund where the glaciers are situated in open neve-like basins which lack large scree slopes above the glacier surface. Given this, we suggest that the Upper Zemmgrund glaciers do not fit with the broad assessment that debris cover will increase over the glacial to paraglacial transition (e.g., Fischer et al., 2021; Fleischer et al., 2021).

The role of aeolian dust in enhancing glacier retreat in the Alps has been disputed and has been linked to lower glacier surface albedo and cryoconite growth. In some instances (e.g., Oerlemans et al., 2009), increased deposition of dust from unvegetated moraines, particularly in years with lower snowpack coverage, has been attributed to accelerated glacier melt. However, the influence of this process is likely restricted by local topography, and in the case of the Upper Zemmgrund, no large unvegetated lateral moraines exist above the 2021 glacier extents nor do large topographically-shielded areas suited to dust accumulation exist. Additionally, non-local sources e.g., Saharan dust events occurring prior to the melt season, have been linked to earlier snowpack melt due to reducing the surface albedo when exposed, exacerbating the vulnerability of glaciers to high summer melt (Di Mauro et al., 2019; Di Mauro and Fugazza, 2022). It is likely that most glaciers in the Alps are trending towards earlier snowpack melt, hence it is hard to differentiate between increased temperatures and the role of aeolian dust. However, aeolian dust events are not a new phenomenon and in conjunction with our observations of only a slight increase of debris cover, it is likely that the effect of aeolian dust on glacier melt in the Zemmgrund is subdued.

5.3. *Paraglacial transition*

The geomorphological and sedimentological assemblages resulting from a transition towards glacial downwasting and retreat have recently been described as a 'dying glacier landsystem' based upon the retreat of Pasterze Glacier, Austria (Le Heron et al., 2022). Situated in a confined valley prone to rockfalls and avalanches, the topographic setting of the Pasterze Glacier is not directly comparable to the Upper Zemmgrund, with the lower portion of the Pasterze Glacier having now arguably transitioned into a downwasting mass of dead ice. The primary cause of disintegration may predominantly be attributed to the disconnection from the accumulation area; however, this positive feedback is amplified by the role of meltwater, often leading to incised canyon formation resulting in collapse structures, and accelerated melting from pro- and supraglacial lake formation. Additionally, a reduction in ice-flow velocity has resulted in increased circular tension collapse structures in low-velocity areas, primarily at the glacier terminus (Stocker-Waldhuber et al., 2017), with these collapse structures often resulting in the ponding of meltwater which can drive further disintegration due to a reduced surface albedo. Similarly, the influence of meltwater and debris cover on rapid de-icing has also been observed under continuous permafrost conditions in the high Arctic. For example, Lukas et al. (2005) described the development of instabilities such as steep frontal slopes and collapse of englacial meltwater channels which triggered self-reinforcing cycles of enhanced surface debris removal and ablation (termed the "cycle of degradation"). Hence, whilst it is clear that the primary drivers of disintegration are a lack of glacier replenishment, it is apparent that debris remobilisation and meltwater pooling or incision play a significant role in amplifying the rate and extent of glacier degradation.

In contrast to the above examples, the Upper Zemmgrund glaciers show no evidence of large debris bands, debris flows or rockfall deposits,

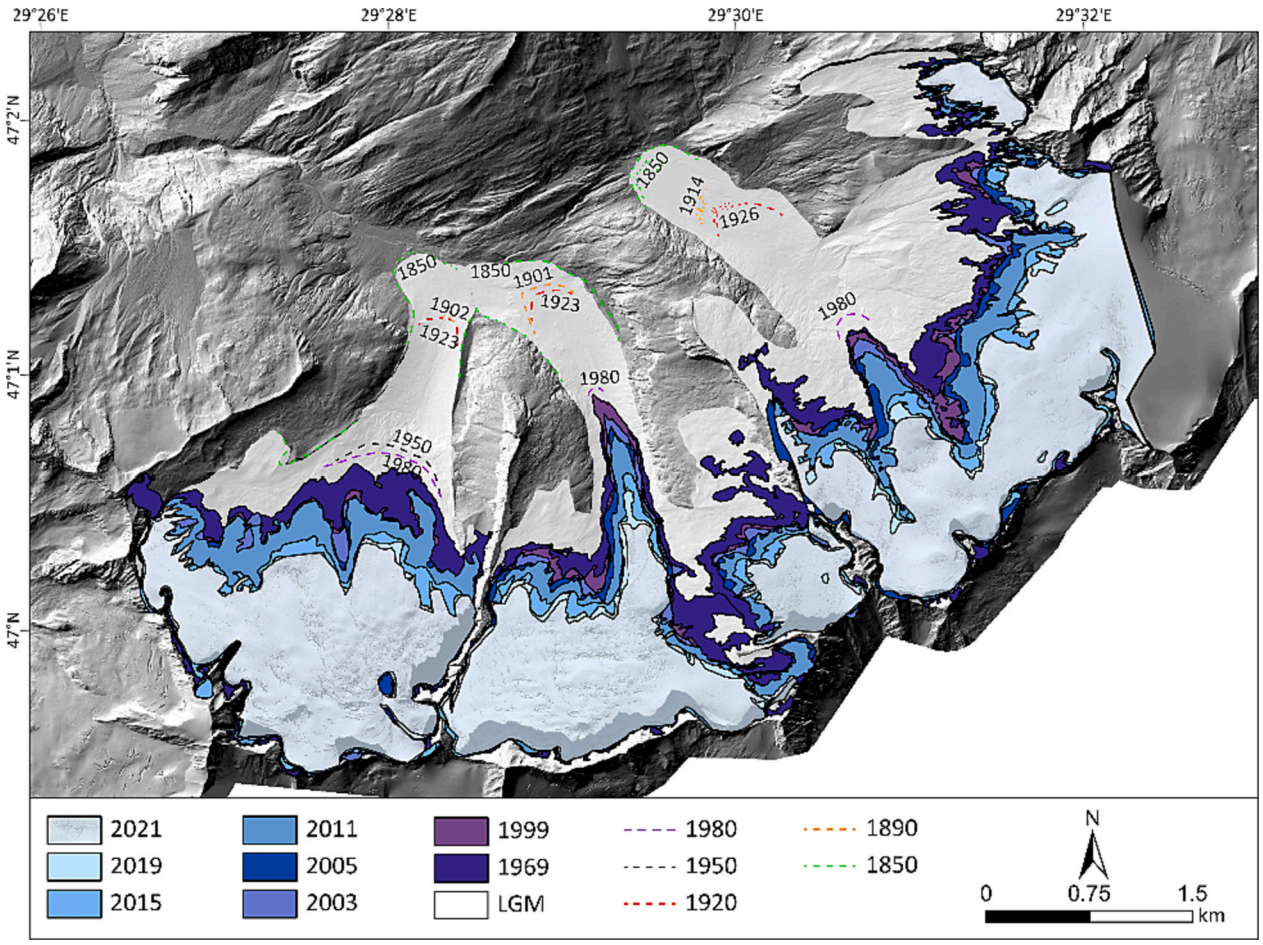

Fig. 9. Temporal changes in glacier extent in the Upper Zemmgrund between 1850 and 2021. Moraine dating is assumed to reflect the position of the ice margin at the respective date. Data obtained from Pindur and Heuberger (2008) for the ~1890 and ~1920 formed moraines is used to group the moraines identified in the result section by this study to their respective locality-wide advances. Glacier extent mapping utilises manually delineated outlines produced by this study for 2003, 2005, 2015, 2019 and 2021. Data for the 1850, 1969, 1999 and 2011 glacier positions is obtained from the Austrian Glacier Inventory.

with debris cover showing very little increase over time (Table 4). It is possible that either the glaciers in the Upper Zemmgrund have not yet reached a disintegration scenario, or that the diagnostic symptoms of glacier disintegration may vary widely due to factors such as strong topographic controls on debris cover (see Section 5.2.2), and therefore the Upper Zemmgrund and other cleaner ice glaciers may not mirror the characteristics of a debris-covered glacier's demise. Of the three glaciers, Hornkees may be the most at risk from disintegration in the near term due to rapid downwasting over a small ice fall where the glacier snout extends down to the valley floor. Following mapping, the development of a circular tension fault at the snout of Hornkees in 2020 provides evidence of a roof collapse over an englacial or subglacial meltwater channel, which does appear to follow the characteristic patterns of glacier degradation observed elsewhere (Lukas et al., 2005; Le Heron et al., 2022).

Circular tension cracks have been observed as early as the 1950s (e.g., Odell, 1960), and whilst these features alone are not evidence of disintegration, their increased prevalence is a result of higher ablation rates (Kellerer-Pirklbauer and Kulmer, 2019). The circular tension crack at Hornkees subsequently collapsed in 2021, along with an additional circular crack closer to the terminus, which merged in 2022 to form a supraglacial lake (Fig. 11). The lake appears to have partially drained in 2022 but could continue to pose a downstream hazard (Fig. 11). The collapse of two circular tension cracks within a year suggests that Hornkees is undergoing disintegration as no such features were previously observed across our satellite imagery observation period (1971 to 2019). The cycle of collapse structure formation observed at Hornkees shares similarities with other retreating glaciers (e.g., Gulley and Benn, 2007; Benn et al., 2017), following a cycle of (1) subglacial or englacial cavity development, (2) formation of circular tension features at the glacier surface and (3) roof collapse (Fig. 11). However, at Hornkees the expansion/growth of a new lake or exposure of pre-existing subglacial lake, which does not occur at all collapse sites, reduces the surface albedo, and will likely accelerate retreat at its terminus. Hence, it is clear that the Upper Zemmgrund landscape has transitioned away from one of active glacial modification to a dying glacier landsystem, despite some dissimilarities with the proposed landsystem model, and will eventually become primarily dominated by paraglacial processes (Knight and Harrison, 2014).

5.4. Future scenarios

Observed rates of retreat in the Zemmgrund are broadly consistent with Alps-wide trends in glacier retreat when compared to the corresponding size classes in European glacier inventories (e.g., Lambrecht and Kuhn, 2007; Gardent et al., 2014; Paul et al., 2020). Across the Alps, a westward trend of increasing rates of mass and area loss is apparent (Gardent et al., 2014; Sommer et al., 2020), with the Eastern Alps documenting lower rates of glacier change and a lower sensitivity to changing air temperatures (Braithwaite et al., 2013). For example, between ~1969 and 2005, glaciers within the 1–5 km^2 class in the French Alps lost 36.1 % of their area, whereas the Zemmgrund glaciers in the

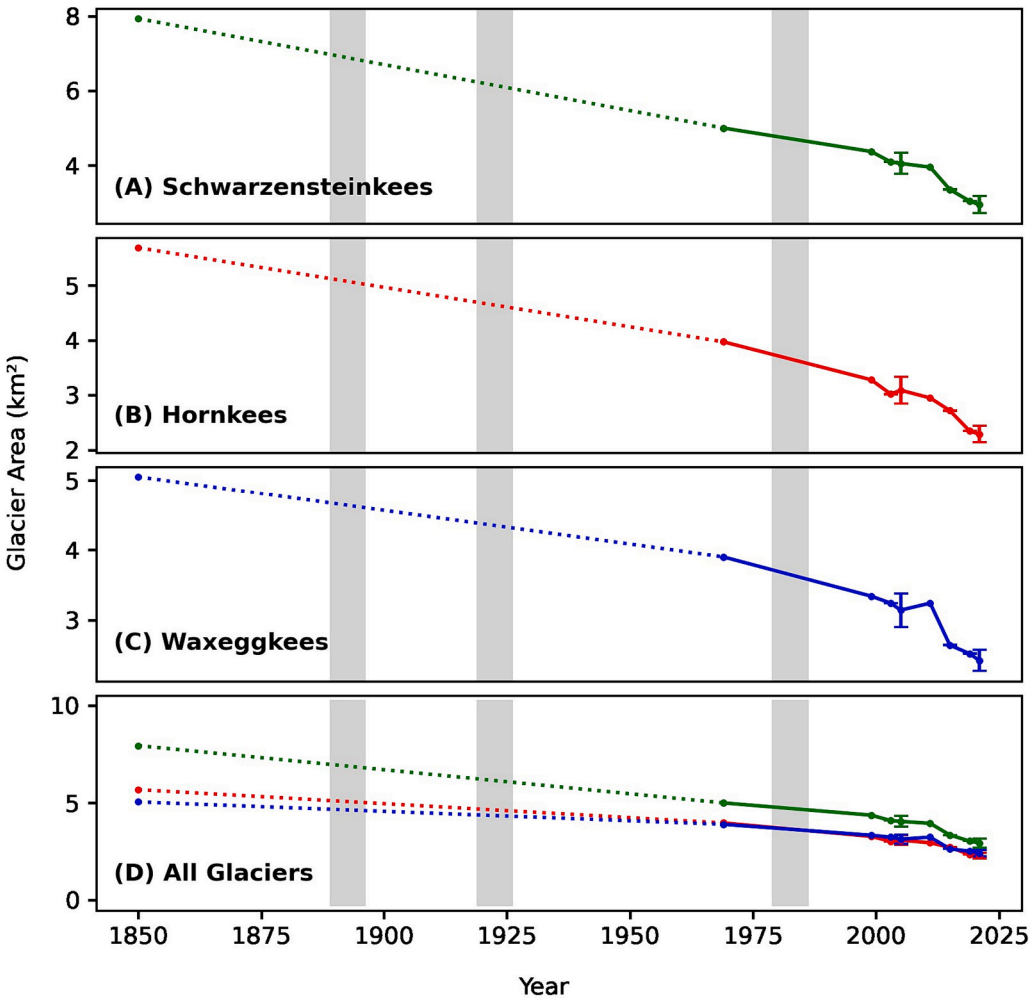

Fig. 10. Glacier change in the Zemmgrund (1850 to 2021). Error bars reflect the minimum and maximum possible extents of glacier area at each date. The dotted line between 1850 and 1969 represents the broad trend of glacier retreat, with the known periods of glacier advance marked by grey bars.

Table 3
Changes in crevassed area from 1971 to 2019 for the Upper Zemmgrund glaciers. The data has been obtained by calculating the number of shapefiles produced as part of the geomorphological mapping.

Year	Number of crevasses	Crevasses (per km^2)
	Schwarzensteinkees Glacier	
2019	1992	694.08
2003	2529	645.15
1971	2450	522.39
	Hornkees Glacier	
2019	1256	532.2
2003	1412	455.48
1971	1458	367.25
	Waxeggkees Glacier	
2019	1296	524.7
2003	1065	331.78
1971	703	179.8

Table 4
Changes in supraglacial debris cover from 1971 to 2019 for the Upper Zemmgrund glaciers. The debris cover has been calculated from the geometries of supraglacial debris shapefiles produced from the geomorphological mapping.

Year	Debris cover (km^2)	Debris cover as a percentage of glacier area
	Schwarzensteinkees Glacier exc. Mörchnerkees	
2019	0.18	6.45 %
2003	0.07	1.75 %
1971	0.04	0.88 %
	Hornkees Glacier	
2019	0.08	3.42 %
2003	0.12	3.87 %
1971	0.1	2.58 %
	Waxeggkees Glacier	
2019	0.04	1.48 %
2003	0.07	2.10 %
1971	0.04	0.91 %

Eastern Alps range between 19 and 26 % (Gardent et al., 2014). When compared within Austria, glaciers between 1 and 5 km^2 in the Ötztal Alps (−11.4 %) recorded a lower average retreat rate than the Zemmgrund (−13 to 17 %) during the period between 1969 and 99. However, this period is complicated by a documented advance in the 1980s, only recorded in Hornkees foreland (Fig. 5), and when compared to a period of known net retreat (1997–06), glaciers in the Zemmgrund have experienced slightly lower rates of retreat than the Ötztal Alps. Similar to the proposed explanation for retreat differences between the Western and Eastern Alps (Sommer et al., 2020), it is likely that the lower retreat rates in the Zemmgrund can be explained by the lack of ice at lower elevations and the presence of more sheltered conditions. More broadly,

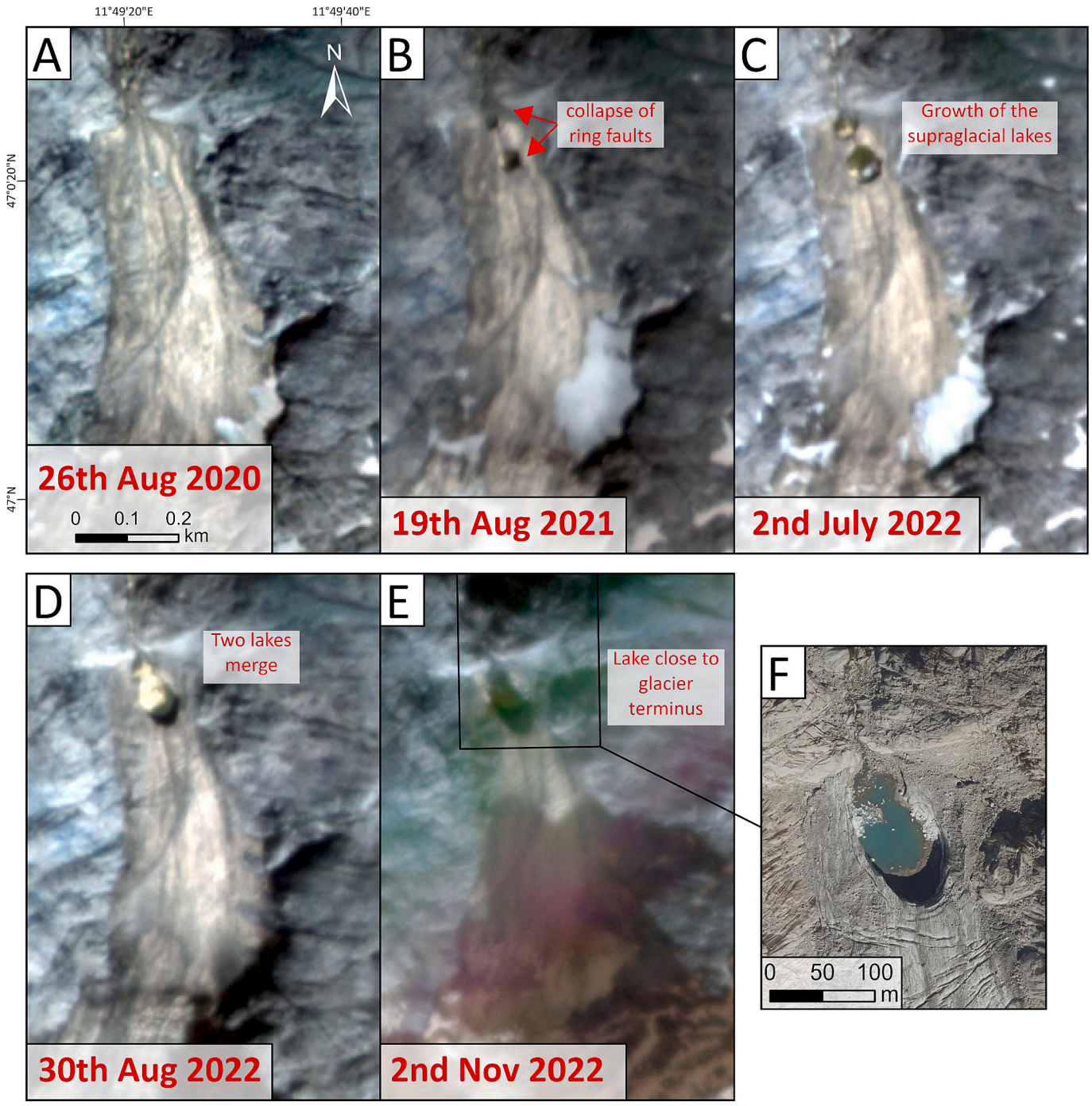

Fig. 11. The evolution and collapse of circular tension crack structures at Hornkees terminus from Planet SuperDove imagery (resolution of 3 m) (Planet Team, 2017). (A) Imagery of the tension crack in 2020 during the summer before its collapse. (B) The collapse of two circular tension crack structures on Hornkees, with the larger supraglacial pond corresponding with crevasse patterns seen at Hornkees terminus in the 2019 mapping (Fig. 5). (C) Continued growth of the two supraglacial ponds (D) The expansion of the two ponds to form a larger lake close to the terminus, although the water level has slightly decreased implying a potential drainage event. (E) The last documentation of the lake before winter, with the lake appearing to have not drained. (F) A high-resolution 2022 orthophoto showing the collapsed circular tension structure.

the effect of glacier hypsometry can be seen in other rapidly changing latitudes, for example, trends of increasingly negative mass balance in Svalbard have been linked to lower elevation glaciers (Nuth et al., 2007), and variation in ice cap outlet retreat rates show similar trends in mainland Norway (Andreassen et al., 2020). Ultimately, it is easy to link broad trends of increased temperature to growing vulnerability of glacier ice at higher elevations, however, our work in the Zemmgrund demonstrates that uniform climate change within a single valley does not always result in a uniform style of retreat between neighbouring glaciers.

Future landscape evolution in the Upper Zemmgrund can be anticipated from long-term observations of past changes. A best-case estimate of glacier longevity based upon linear extrapolation of glacier retreat rates between 2015 and 2021 would predict the disappearance of Schwarzensteinkees in 43 years, Hornkees in 55 years and Waxeggkees in 66 years, without accounting for further projected climatic warming. This remains in accordance with a high-emission scenario (RCP8.5), which predicts the Alps will be primarily ice-free by the end of the 21st

century, with the ELA projected to exceed the maximum elevation of 92 % of European Alpine glaciers (Zekollari et al., 2019; Žebre et al., 2021). The effect of glacier retreat on hydrology is already evident in the Upper Zemmgrund from the reduction in meltwater channel width, implying a reduction in discharge. Consistent with other regions in the Alps, the Zemmbach River is likely to trend towards peak discharge earlier in the year (Haeberli and Hohmann, 2008). The Zemmbach River is partly diverted to feed the Schlegeis Reservoir, and therefore reduced glacier melt input could directly impact both hydropower generation and freshwater availability. In addition, the growing influence of paraglacial processes presents additional hazards, notably an increased risk of mass movements from unconsolidated scree slopes and lateral moraines, thaw-out of permafrost in fractured rock masses (e.g., Krautblatter et al., 2013) and the damming of proglacial lakes (Knight and Harrison, 2014; Zanoner et al., 2017). In the case of the Zemmgrund, the biggest implications of glacier retreat will most likely lead to a reduction in river discharge, increased sediment supply, and flooding due to run-off on surfaces not yet colonised by vegetation.

6. Conclusion

Using a multi-method approach that incorporated satellite imagery, aerial orthophotos, digital elevation models, together with archival photography, artwork and cartography, we investigated the retreat of three neighbouring glaciers in the Upper Zemmgrund, Austria. With this combined record and informed by local field observations, we collated detailed geomorphological maps of both glacier forefields and glacier surface features to reconstruct the rate, extent, and dynamics of glacier retreat since the Little Ice Age (LIA) maximum ~1850. We find that glacier surface area in the Upper Zemmgrund has decreased by 59 %, from an LIA maximum of 18.7 km^2 to 7.7 km^2 in 2021, driven primarily by increasing summer temperatures. Together with collapses at the proglacial margin, no evidence of any glacier advance since the 1980s, development of circular tension cracks, and minor increased surface debris cover by area (+2.3 %; 1971–2019) suggest a general transition towards glacier disintegration in the area. However, we find significant variability in intra-catchment retreat rates because of locally varying characteristics, such as hypsometry and glacier size that are important factors which must be accounted for in regional predictions of glacier retreat. Nonetheless, at current rates of retreat, the Upper Zemmgrund is likely to be ice-free within 40–60 years. Ongoing glacier retreat will have important implications for hazard management and green energy production in the region, and potentially a decline in freshwater availability following glacier recession. This study demonstrates the value of a multi-method approach to mapping glacier recession and provides a blueprint readily adaptable to other contexts globally.

CRediT authorship contribution statement

H. Wytiahlowsky: Conceptualization, Formal analysis, Investigation, Methodology, Visualization, Writing – original draft, Writing – review & editing. **M.E. Busfield:** Conceptualization, Supervision, Writing – review & editing. **A.J. Hepburn:** Writing – review & editing. **S. Lukas:** Writing – review & editing.

Declaration of competing interest

The authors declare that they have no known competing financial interests or personal relationships that could have appeared to influence the work reported in this paper.

Data availability

Data will be made available on request.

Acknowledgements

This research was carried out by HW as part of a Bachelor of Science degree in the Department of Geography and Earth Sciences at Aberystwyth University. We thank Matteo Spagnolo and an anonymous reviewer for their constructive comments on this manuscript. We thank Land Tirol for making elevation data and orthophotos open access. The staff at the archives of the Austrian Alpine Club (Österreicher Alpenverein), notably Martin Achrainer, are thanked for their hospitality in Innsbruck and for invaluable help in tracking down crucial historical documents. The staff at the DAV Berliner Hütte are warmly thanked for their hospitality and logistical support of our research over numerous consecutive field seasons. We are grateful to Cianna Wyshnytzky, Miriam Dühnforth, and Barbara and Harald Krenn for helpful discussions in the field and during data analyses. Finally, SL thanks the Quaternary Research Association and MB thanks the Aberystwyth University Research Fund for financial support for work on parallel projects that enabled joint fieldwork to be undertaken.

References

Abermann, J., Lambrecht, A., Fischer, A., Kuhn, M., 2009. Quantifying changes and trends in glacier area and volume in the Austrian Ötztal Alps (1969-1997-2006). Cryosphere 3, 205–215. https://doi.org/10.5194/tc-3-205-2009.

Andreassen, L.M., Elvehøy, H., Kjøllmoen, B., Belart, J.M.C., 2020. Glacier change in Norway since the 1960s – an overview of mass balance, area, length and surface elevation changes. J. Glaciol. 66, 313–328. https://doi.org/10.1017/jog.2020.10.

Azzoni, R.S., Fugazza, D., Zennaro, M., Zucali, M., D'Agata, C., Maragno, D., Cernuschi, M., Smiraglia, C., Diolaiuti, G.A., 2017. Recent structural evolution of Forni Glacier tongue (Ortles-Cevedale Group, Central Italian Alps). J. Maps 13, 870–878. https://doi.org/10.1080/17445647.2017.1394227.

Ballantyne, C.K., 2002. Paraglacial geomorphology. Quat. Sci. Rev. 21, 1935–2017. https://doi.org/10.1016/S0277-3791(02)00005-7.

Benn, D.I., Evans, D.J.A., 2010. Glaciers and Glaciation. Hodder Education, London.

Benn, D.I., Thompson, S., Gulley, J., Mertes, J., Luckman, A., Nicholson, L., 2017. Structure and evolution of the drainage system of a Himalayan debris-covered glacier, and its relationship with patterns of mass loss. Cryosphere 11, 2247–2264. https://doi.org/10.5194/tc-11-2247-2017.

Betz-Nutz, S., Heckmann, T., Haas, F., Becht, M., 2023. Development of the morphodynamics on little ice age lateral moraines in 10 glacier forefields of the Eastern Alps since the 1950s. Earth Surf. Dyn. 11, 203–226. https://doi.org/10.5194/esurf-11-203-2023.

Braithwaite, R.J., Raper, S.C.B., Candela, R., 2013. Recent changes (1991–2010) in glacier mass balance and air temperature in the European Alps. Ann. Glaciol. 54, 139–146. https://doi.org/10.3189/2013AoG63A285.

Brunner, K., Rentsch, H., 2002. The behavior of the Waxeggkees in the Zillertal Alps from1950 to 2000. Z. Fur Gletscherkd. Glazialgeol. 38 (1), 63–69.

Buckel, J., Otto, J.-C., 2018. The Austrian Glacier Inventory GI 4 (2015) in ArcGis (Shapefile) Format. https://doi.org/10.1594/PANGAEA.887415.

Chandler, B.M.P., Lovell, H., Boston, C.M., Lukas, S., Barr, I.D., Benediktsson, Í.Ö., Benn, D.I., Clark, C.D., Darvill, C.M., Evans, D.J.A., Ewertowski, M.W., Loibl, D., Margold, M., Otto, J.-C., Roberts, D.H., Stokes, C.R., Storrar, R.D., Stroeven, A.P., 2018. Glacial geomorphological mapping: a review of approaches and frameworks for best practice. Earth Sci. Rev. 185, 806–846. https://doi.org/10.1016/j.earscirev.2018.07.015.

Citterio, M., Diolaiuti, G., Smiraglia, C., D'agata, C., Carnielli, T., Stella, G., Siletto, G.B., 2007. The fluctuations of italian glaciers during the last century: a contribution to knowledge about alpine glacier changes. Geogr. Ann. A: Phys. Geogr. 89, 167–184. https://doi.org/10.1111/j.1468-0459.2007.00316.x.

Curry, A.M., Cleasby, V., Zukowskyj, P., 2006. Paraglacial response of steep, sediment-mantled slopes to post-'Little Ice Age' glacier recession in the central Swiss Alps. J. Quat. Sci. 21 (3), 211–225. https://doi.org/10.1002/jqs.954.

De Angelis, H., 2014. Hypsometry and sensitivity of the mass balance to changes in equilibrium-line altitude: the case of the Southern Patagonia Icefield. J. Glaciol. 60, 14–28. https://doi.org/10.3189/2014JoG13J127.

DeBeer, C.M., Sharp, M.J., 2007. Recent changes in glacier area and volume within the southern Canadian Cordillera. Ann. Glaciol. 46, 215–221. https://doi.org/10.3189/172756407782871710.

Di Mauro, B., Fugazza, D., 2022. Pan-Alpine glacier phenology reveals lowering albedo and increase in ablation season length. Remote Sens. Environ. 279, 113119 https://doi.org/10.1016/j.rse.2022.113119.

Di Mauro, B., Garzonio, R., Rossini, M., Filippa, G., Pogliotti, P., Galvagno, M., Morra di Cella, U., Migliavacca, M., Baccolo, G., Clemenza, M., Delmonte, B., Maggi, V., Dumont, M., Tuzet, F., Lafaysse, M., Morin, S., Cremonese, E., Colombo, R., 2019. Saharan dust events in the European Alps: role in snowmelt and geochemical characterization. Cryosphere 13, 1147–1165. https://doi.org/10.5194/tc-13-1147-2019.

Dusik, J.M., Neugirg, F., Haas, F., 2019. Slope wash, gully erosion and debris flows on lateral moraines in the Upper Kaunertal, Austria. In: Geomorphology of Proglacial

Systems: Landform and Sediment Dynamics in Recently Deglaciated Alpine Landscapes, pp. 177–196.
Eichel, J., Draebing, D., Meyer, N., 2018. From active to stable: Paraglacial transition of Alpine lateral moraine slopes. Land Degrad. Dev. 29, 4158–4172. https://doi.org/10.1002/ldr.3140.
Ender, T., 1841. Der Keesdboden am Schwarzen Stein. [water colour]. Austrian Private Collection. Available at: https://upload.wikimedia.org/wikipedia/commons/a/af/Thomas_Ender_-_Der_Keesboden_am_Schwarzen_Stein.jpg. (Accessed October 2023).
Ewertowski, M.W., Evans, D.J.A., Roberts, D.H., Tomczyk, A.M., Ewertowski, W., Pleksot, K., 2019. Quantification of historical landscape change on the foreland of a receding polythermal glacier, Hørbyebreen, Svalbard. Geomorphology 325, 40–54. https://doi.org/10.1016/j.geomorph.2018.09.027.
Fiddes, J., Gruber, S., 2014. TopoSCALE v.1.0: downscaling gridded climate data in complex terrain. Geosci. Model Dev. 7, 387–405. https://doi.org/10.5194/gmd-7-387-2014.
Fischer, A., Seiser, B., Stocker Waldhuber, M., Mitterer, C., Abermann, J., 2015. Tracing glacier changes in Austria from the Little Ice Age to the present using a lidar-based high-resolution glacier inventory in Austria. Cryosphere 9, 753–766. https://doi.org/10.5194/tc-9-753-2015.
Fischer, A., Schwaizer, G., Seiser, B., Helfricht, K., Stocker-Waldhuber, M., 2021. High-resolution inventory to capture glacier disintegration in the Austrian Silvretta. Cryosphere 15, 4637–4654. https://doi.org/10.5194/tc-15-4637-2021.
Fleischer, F., Otto, J.-C., Junker, R.R., Hölbling, D., 2021. Evolution of debris cover on glaciers of the Eastern Alps, Austria, between 1996 and 2015. Earth Surf. Process. Landf. 46, 1673–1691. https://doi.org/10.1002/esp.5065.
Gardent, M., Rabatel, A., Dedieu, J.-P., Deline, P., 2014. Multitemporal glacier inventory of the French Alps from the late 1960s to the late 2000s. Glob. Planet. Change 120, 24–37. https://doi.org/10.1016/j.gloplacha.2014.05.004.
Gharehchahi, S., Ballinger, T.J., Jensen, J.L.R., Bhardwaj, A., Sam, L., Weaver, R.C., Butler, D.R., 2021. Local- and regional-scale forcing of glacier mass balance changes in the Swiss Alps. Remote Sens. (Basel) 13, 1949. https://doi.org/10.3390/rs13101949.
Glasser, N.F., Holt, T.O., Evans, Z.D., Davies, B.J., Pelto, M., Harrison, S., 2016. Recent spatial and temporal variations in debris cover on Patagonian glaciers. Geomorphology 273, 202–216. https://doi.org/10.1016/j.geomorph.2016.07.036.
Gobiet, A., Kotlarski, S., Beniston, M., Heinrich, G., Rajczak, J., Stoffel, M., 2014. 21st century climate change in the European Alps—a review. Sci. Total Environ. 493, 1138–1151. https://doi.org/10.1016/j.scitotenv.2013.07.050.
Goodsell, B., Hambrey, M.J., Glasser, N.F., 2005. Debris transport in a temperate valley glacier: Haut Glacier d'Arolla, Valais, Switzerland. J. Glaciol. 51, 139–146. https://doi.org/10.3189/172756505781829647.
Groß, G., Patzelt, G., 2015. The Austrian Glacier Inventory for the Little Ice Age Maximum (GI LIA) in ArcGIS (shapefile) format. In supplement to: Fischer, Andrea; Seiser, Bernd; Stocker-Waldhuber, Martin; Mitterer, Christian; Abermann, Jakob (2015): tracing glacier changes in Austria from the Little Ice Age to the present using a lidar-based high-resolution glacier inventory in Austria. Cryosphere 9 (2), 753–766. https://doi.org/10.5194/tc-9-753-2015 (doi: 10.1594/PANGAEA.844987).
Grove, J.M., Switsur, R., 1994. Glacial geological evidence for the medieval warm period. In: Hughes, M.K., Diaz, H.F. (Eds.), The Medieval Warm Period. Springer, Netherlands, Dordrecht, pp. 143–169. https://doi.org/10.1007/978-94-011-1186-7_2.
Gulley, J., Benn, D.I., 2007. Structural control of englacial drainage systems in Himalayan debris-covered glaciers. J. Glaciol. 53, 399–412. https://doi.org/10.3189/002214307783258378.
Haeberli, W., Hohmann, R., 2008. Climate, glaciers and permafrost in the Swiss Alps 2050: scenarios, consequences and recommendations. In: Haeberli, W., Hohmann, R. (Eds.), Climate, Glaciers and Permafrost in the Swiss Alps 2050: Scenarios, Consequences and Recommendations. In: 9th International Conference on Permafrost, Fairbanks, Alaska, 29 June 2008–3 July 2008, 607–612. Presented at the 9th International Conference on Permafrost, University of Zurich, Fairbanks, Alaska, pp. 607–612. https://doi.org/10.5167/uzh-6025.
Hannesdóttir, H., Björnsson, H., Pálsson, F., Aðalgeirsdóttir, G., Guðmundsson, S., 2015. Variations of southeast vatnajökull ice cap (Iceland) 1650–1900 and reconstruction of the glacier surface geometry at the little ice age maximum. Geogr. Ann. A: Phys. Geogr. 97, 237–264. https://doi.org/10.1111/geoa.12064.
Hock, R., Rasul, G., Adler, C., Cáceres, B., Gruber, S., Hirabayashi, Y., Jackson, M., Kääb, A., Kang, S., Kutuzov, S., Milner, A., Molau, U., Morin, S., Orlove, B., Steltzer, H., Allen, S., Arenson, L., Baneerjee, S., Barr, I., Bórquez, R., Brown, L., Cao, B., Carey, M., Cogley, G., Fischlin, A., de Sherbinin, A., Eckert, N., Geertsema, M., Hagenstad, M., Honsberg, M., Hood, E., Huss, M., Jimenez Zamora, E., Kotlarski, S., Lefeuvre, P.-M., López Moreno, J.I., Lundquist, J., McDowell, G., Mills, S., Mou, C., Nepal, S., Noetzli, J., Palazzi, E., Pepin, N., Rixen, C., Shahgedanova, M., Skiles, S.M., Vincent, C., Viviroli, D., Weyhenmeyer, G., Sherpa, P.Y., Weyer, N., Wouters, B., Yasunari, T.J., You, Q., Zhang, Y., 2019. High mountain areas. In: Pörtner, H.-O., Roberts, D.C., Masson-Delmotte, V., Zhai, P., Tignor, M., Poloczanska, E., Mintenbeck, K., Nicolai, M., Okem, A., Petzold, J., Rama, B., Weyer, N. (Eds.), The Ocean and Cryosphere in a Changing Climate. Intergovernmental Panel on Climate Change (pp. 2-1-2–90).
Hugonnet, R., McNabb, R., Berthier, E., Menounos, B., Nuth, C., Girod, L., Farinotti, D., Huss, M., Dussaillant, I., Brun, F., Kääb, A., 2021. Accelerated global glacier mass loss in the early twenty-first century. Nature 592, 726–731. https://doi.org/10.1038/s41586-021-03436-z.
Humlum, O., 1978. Genesis of layered lateral moraines. Dan. J. Geogr. 77, 65–72. https://doi.org/10.1080/00167223.1978.10649094.
Jiskoot, H., Curran, C.J., Tessler, D.L., Shenton, L.R., 2009. Changes in Clemenceau Icefield and Chaba Group glaciers, Canada, related to hypsometry, tributary detachment, length–slope and area–aspect relations. Ann. Glaciol. 50, 133–143. https://doi.org/10.3189/172756410790595796.
Johannes, B., 1919. Berliner Hütte (Sektion Berlin) in den Zillertaler Alpen im Jahre 1879 aus Zeitschrift des Deutschen und Oesterreichischen Alpenvereins 1919 Band 50. Available at: https://commons.wikimedia.org/wiki/File:Berliner_H%C3%BCtte_1879_Zillertaler_Alpen.jpg. (Accessed October 2023).
Jouvet, G., 2023. Inversion of a Stokes glacier flow model emulated by deep learning. J. Glaciol. 69, 13–26. https://doi.org/10.1017/jog.2022.41.
Juen, M., Mayer, C., Lambrecht, A., Han, H., Liu, S., 2014. Impact of varying debris cover thickness on ablation: a case study for Koxkar Glacier in the Tien Shan. Cryosphere 8, 377–386. https://doi.org/10.5194/tc-8-377-2014.
Keiler, M., Knight, J., Harrison, S., 2010. Climate change and geomorphological hazards in the eastern European Alps. Proc. R. Soc. A: Math. Phys. Eng. Sci. 368, 2461–2479. https://doi.org/10.1098/rsta.2010.0047.
Kellerer-Pirklbauer, A., Kulmer, B., 2019. The evolution of brittle and ductile structures at the surface of a partly debris-covered, rapidly thinning and slowly moving glacier in 1998–2012 (Pasterze Glacier, Austria). Earth Surf. Process. Landf. 44, 1034–1049. https://doi.org/10.1002/esp.4552.
Knight, J., Harrison, S., 2014. Glacial and paraglacial environments. Geogr. Ann. A: Phys. Geogr. 96, 241–244. https://doi.org/10.1111/geoa.12058.
Krautblatter, M., Funk, D., Günzel, F.K., 2013. Why permafrost rocks become unstable: a rock–ice-mechanical model in time and space. Earth Surf. Process. Landf. 38, 876–887. https://doi.org/10.1002/esp.3374.
Kuhn, M., Markl, G., Kaser, G., Nickus, U., Obleitner, F., Schneider, H., 1985. Fluctuations of climate and mass balance: different responses of two adjacent glaciers. Z. Gletscherkd. Glazialgeol. 21, 409–416.
Kuhn, M., Lambrecht, A., Abermann, J., 2015. The Austrian glacier inventory GI 2, 1998, in ArcGIS (shapefile) format. In supplement to: Fischer, Andrea; Seiser, Bernd; Stocker-Waldhuber, Martin; Mitterer, Christian; Abermann, Jakob (2015): tracing glacier changes in Austria from the Little Ice Age to the present using a lidar-based high-resolution glacier inventory in Austria. Cryosphere 9 (2), 753–766. https://doi.org/10.5194/tc-9-753-2015 (doi: 10.1594/PANGAEA.844984).
Lambrecht, A., Kuhn, M., 2007. Glacier changes in the Austrian Alps during the last three decades, derived from the new Austrian glacier inventory. Ann. Glaciol. 46, 177–184. https://doi.org/10.3189/172756407782871341.
Le Heron, D.P., Kettler, C., Wawra, A., Schöpfer, M., Grasemann, B., 2022. The sedimentological death mask of a dying glacier. Depos. Rec. 8, 992–1007. https://doi.org/10.1002/dep2.205.
Lukas, S., 2012. Processes of annual moraine formation at a temperate alpine valley glacier: insights into glacier dynamics and climatic controls. Boreas 41, 463–480. https://doi.org/10.1111/j.1502-3885.2011.00241.x.
Lukas, S., Busfield, M.E., 2017, April. Solving the puzzle of an isolated high-Alpine drumlin: Hornkees, Austria. In: EGU General Assembly Conference Abstracts, p. 8281.
Lukas, S., Sass, O., 2011. The formation of Alpine lateral moraines inferred from sedimentology and radar reflection patterns: a case study from Gornergletscher, Switzerland. Geol. Soc. Spec. Publ. 354, 77–92. https://doi.org/10.1144/SP354.5.
Lukas, S., Nicholson, L.I., Ross, F.H., Humlum, O., 2005. Formation, meltout processes and landscape alteration of high-arctic ice-cored moraines—examples from Nordenskiold Land, Central Spitsbergen. Polar Geogr. 29, 157–187. https://doi.org/10.1080/789610198.
Lukas, S., Graf, A., Coray, S., Schlüchter, C., 2012. Genesis, stability and preservation potential of large lateral moraines of Alpine valley glaciers – towards a unifying theory based on Findelengletscher, Switzerland. Quat. Sci. Rev. 38, 27–48. https://doi.org/10.1016/j.quascirev.2012.01.022.
Luterbacher, J., Werner, J.P., Smerdon, J.E., Fernández-Donado, L., González-Rouco, F. J., Barriopedro, D., Ljungqvist, F.C., Büntgen, U., Zorita, E., Wagner, S., Esper, J., McCarroll, D., Toreti, A., Frank, D., Jungclaus, J.H., Barriendos, M., Bertolin, C., Bothe, O., Brázdil, R., Camuffo, D., Dobrovolný, P., Gagen, M., García-Bustamante, E., Ge, Q., Gómez-Navarro, J.J., Guiot, J., Hao, Z., Hegerl, G.C., Holmgren, K., Klimenko, V.V., Martín-Chivelet, J., Pfister, C., Roberts, N., Schindler, A., Schurer, A., Solomina, O., von Gunten, L., Wahl, E., Wanner, H., Wetter, O., Xoplaki, E., Yuan, N., Zanchettin, D., Zhang, H., Zerefos, C., 2016. European summer temperatures since Roman times. Environ. Res. Lett. 11, 024001 https://doi.org/10.1088/1748-9326/11/2/024001.
Mahaney, W.C., Hancock, R.G.V., Melville, H., 2011. Late glacial retreat and Neoglacial advance sequences in the Zillertal Alps, Austria. Geomorphology 130, 312–326. https://doi.org/10.1016/j.geomorph.2011.04.013.
Marlin, C., Tolle, F., Griselin, M., Bernard, E., Saintenoy, A., Quenet, M., Friedt, J.-M., 2017. Change in geometry of a high Arctic glacier from 1948 to 2013 (Austre Lovénbreen, Svalbard). Geogr. Ann. A: Phys. Geogr. 99, 115–138. https://doi.org/10.1080/04353676.2017.1285203.
Nussbaumer, S.U., Zumbühl, H.J., 2012. The Little Ice Age history of the Glacier des Bossons (Mont Blanc massif, France): a new high-resolution glacier length curve based on historical documents. Clim. Change 111, 301–334. https://doi.org/10.1007/s10584-011-0130-9.
Nuth, C., Kohler, J., Aas, H.F., Brandt, O., Hagen, J.O., 2007. Glacier geometry and elevation changes on Svalbard (1936–90): a baseline dataset. Ann. Glaciol. 46, 106–116. https://doi.org/10.3189/172756407782871440.
Odell, N.E., 1960. The mountains and glaciers of New Zealand. J. Glaciol. 3, 739–744. https://doi.org/10.3189/S0022143000018049.
Oerlemans, J., Giesen, R.H., Broeke, M.R.V.D., 2009. Retreating alpine glaciers: increased melt rates due to accumulation of dust (Vadret da Morteratsch,

Switzerland). J. Glaciol. 55, 729–736. https://doi.org/10.3189/002214309789470969.
Patzelt, G., 1980. The Austrian Glacier Inventory: Status and First Results [WWW Document]. EPIC3Bremerhaven, IAHS Publication. URL. https://epic.awi.de/id/eprint/32383/ (accessed 6.17.23).
Patzelt, G., 2015. The Austrian glacier inventory GI 1, 1969, in ArcGIS (shapefile) format. In supplement to: Fischer, Andrea; Seiser, Bernd; Stocker-Waldhuber, Martin; Mitterer, Christian; Abermann, Jakob (2015): tracing glacier changes in Austria from the Little Ice Age to the present using a lidar-based high-resolution glacier inventory in Austria. Cryosphere 9 (2), 753–766. https://doi.org/10.5194/tc-9-753-2015 (doi: 10.1594/PANGAEA.844983).
Paul, F., Mölg, N., 2014. Hasty retreat of glaciers in northern Patagonia from 1985 to 2011. J. Glaciol. 60, 1033–1043. https://doi.org/10.3189/2014JoG14J104.
Paul, F., Rastner, P., Azzoni, R.S., Diolaiuti, G., Fugazza, D., Le Bris, R., Nemec, J., Rabatel, A., Ramusovic, M., Schwaizer, G., Smiraglia, C., 2020. Glacier shrinkage in the Alps continues unabated as revealed by a new glacier inventory from Sentinel-2. Earth Syst. Sci. Data 12, 1805–1821. https://doi.org/10.5194/essd-12-1805-2020.
Pfeffer, W.T., Sassolas, C., Bahr, D.B., Meier, M.F., 1998. Response time of glaciers as a function of size and mass balance: 2. Numerical experiments. J. Geophys. Res. Solid Earth 103, 9783–9789. https://doi.org/10.1029/98JB00508.
Pindur, P., Heuberger, H., 2008. Zur Holozänen Gletschergeschichte im Zemmgrund in den Zillertalen Alpen, Tirol, Österreich (Ostalpen). Z. Gletscherk. Glazialgeol. 42, 21–89.
Pindur, P., Luzian, R., 2007. The “Upper Zemmgrund” - a geographical overview. BFW Berichte 23–35.
Planet Team, 2017. Planet application program interface: in space for life on earth. San Francisco, CA. https://api.planet.com.
Reid, T.D., Carenzo, M., Pellicciotti, F., Brock, B.W., 2012. Including debris cover effects in a distributed model of glacier ablation. J. Geophys. Res. Atmos. 117 https://doi.org/10.1029/2012JD017795.
Rets, E.P., Durmanov, I.N., Kireeva, M.B., Smirnov, A.M., Popovnin, V.V., 2020. Past ‘peak water’ in the North Caucasus: deglaciation drives a reduction in glacial runoff impacting summer river runoff and peak discharges. Clim. Change 163, 2135–2151. https://doi.org/10.1007/s10584-020-02931-y.
Rettig, L., Lukas, S., Huss, M., 2023. Implications of a rapidly thinning ice margin for annual moraine formation at Gornergletscher, Switzerland. Quat. Sci. Rev. 308, 108085 https://doi.org/10.1016/j.quascirev.2023.108085.
Rott, H., 1993. The glaciers of Europe—glaciers of the Alps. The Austrian Alps. In: Williams Jr., R.S., Ferrigno, J.G. (Eds.), U.S. Geological Survey Professional Paper, vol. 1386-E, pp. E6–E13.
Rounce, D.R., Hock, R., Maussion, F., Hugonnet, R., Kochtitzky, W., Huss, M., Berthier, E., Brinkerhoff, D., Compagno, L., Copland, L., Farinotti, D., Menounos, B., McNabb, R.W., 2023. Global glacier change in the 21st century: every increase in temperature matters. Science 379, 78–83. https://doi.org/10.1126/science.abo1324.
Smith, M.J., Rose, J., Booth, S., 2006. Geomorphological mapping of glacial landforms from remotely sensed data: an evaluation of the principal data sources and an assessment of their quality. Geomorphology 76, 148–165. https://doi.org/10.1016/j.geomorph.2005.11.001.
Sommer, C., Malz, P., Seehaus, T.C., Lippl, S., Zemp, M., Braun, M.H., 2020. Rapid glacier retreat and downwasting throughout the European Alps in the early 21st century. Nat. Commun. 11, 3209. https://doi.org/10.1038/s41467-020-16818-0.
Stocker-Waldhuber, M., Fischer, A., Keller, L., Morche, D., Kuhn, M., 2017. Funnel-shaped surface depressions — indicator or accelerant of rapid glacier disintegration? A case study in the Tyrolean Alps. Geomorphology, Sediment Cascades in Cold Climate Geosystems 287, 58–72. https://doi.org/10.1016/j.geomorph.2016.11.006.
Timár, G., Molnár, G., Székely, B., Biszak, S., Varga, J., Jankó, A., 2006. Zweiten oder Franziszeischen-Landesaufnahme von Salzburg, 1807–1808 [map]: Arcanum.
Williams, R.D., Griffiths, H.M., Carr, J.R., Hepburn, A.J., Gibson, M., Williams, J.J., Irvine-Fynn, T.D.L., 2022. Integrating historical, geomorphological and sedimentological insights to reconstruct past floods: insights from Kea Point, Mt. Cook Village, Aotearoa New Zealand. Geomorphology 398, 108028. https://doi.org/10.1016/j.geomorph.2021.108028.
Wyshnytzky, C.E., 2017. On the Mechanisms of Minor Moraine Formation in High-Mountain Environments of the European Alps (Thesis). Queen Mary University of London.
Wyshnytzky, C., Lukas, S., Groves, J., 2020. Multiple Mechanisms of Minor Moraine Formation in the Schwarzensteinkees Foreland, Austria. https://doi.org/10.1130/2020.2548(10).
Wyshnytzky, C.E., Lukas, S., Groves, J.W.E., 2021. Multiple mechanisms of minor moraine formation in the Schwarzensteinkees foreland, Austria. In: Untangling the Quaternary Period—A Legacy of Stephen C. Porter. Geological Society of America. https://doi.org/10.1130/2020.2548(10).
Zanoner, T., Carton, A., Seppi, R., Carturan, L., Baroni, C., Salvatore, M.C., Zumiani, M., 2017. Little Ice Age mapping as a tool for identifying hazard in the paraglacial environment: the case study of Trentino (Eastern Italian Alps). Geomorphology 295, 551–562. https://doi.org/10.1016/j.geomorph.2017.08.014.
Žebre, M., Colucci, R.R., Giorgi, F., Glasser, N.F., Racoviteanu, A.E., Del Gobbo, C., 2021. 200 years of equilibrium-line altitude variability across the European Alps (1901−2100). Climate Dynam. 56, 1183–1201. https://doi.org/10.1007/s00382-020-05525-7.
Zekollari, H., Huss, M., Farinotti, D., 2019. Modelling the future evolution of glaciers in the European Alps under the EURO-CORDEX RCM ensemble. Cryosphere 13, 1125–1146. https://doi.org/10.5194/tc-13-1125-2019.
Zemp, M., Haeberli, W., Hoelzle, M., Paul, F., 2006. Alpine glaciers to disappear within decades? Geophys. Res. Lett. 33 https://doi.org/10.1029/2006GL026319.
Zemp, M., Paul, F., Hoelzle, M., Haeberli, W., Al, E., 2008. Glacier fluctuations in the European Alps, 1850–2000: an overview and spatio-temporal analysis of available data. In: Orlove, B., Zemp, Michael, Paul, F., Hoelzle, M., Haeberli, W. (Eds.), Glacier Fluctuations in the European Alps, 1850–2000: An Overview and Spatio-Temporal Analysis of Available Data. In: Orlove, B; et al. Darkening Peaks: Glacier Retreat, Science, and Society. Berkeley, US: University of California Press, 152–167. University of California Press, Berkeley, US, pp. 152–167. https://doi.org/10.5167/uzh-9024.
Zemp, M., Frey, H., Gärtner-Roer, I., Nussbaumer, S.U., Hoelzle, M., Paul, F., Haeberli, W., Denzinger, F., Ahlstrøm, A.P., Anderson, B., Bajracharya, S., Baroni, C., Braun, L.N., Cáceres, B.E., Casassa, G., Cobos, G., Dávila, L.R., Granados, H.D., Demuth, M.N., Espizua, L., Fischer, A., Fujita, K., Gadek, B., Ghazanfar, A., Hagen, J. O., Holmlund, P., Karimi, N., Li, Z., Pelto, M., Pitte, P., Popovnin, V.V., Portocarrero, C.A., Prinz, R., Sangewar, C.V., Severskiy, I., Sigurdsson, O., Soruco, A., Usubaliev, R., Vincent, C., 2015. Historically unprecedented global glacier decline in the early 21st century. J. Glaciol. 61, 745–762. https://doi.org/10.3189/2015JoG15J017.
Zemp, M., Huss, M., Thibert, E., Eckert, N., McNabb, R., Huber, J., Barandun, M., Machguth, H., Nussbaumer, S.U., Gärtner-Roer, I., Thomson, L., Paul, F., Maussion, F., Kutuzov, S., Cogley, J.G., 2019. Global glacier mass changes and their contributions to sea-level rise from 1961 to 2016. Nature 568, 382–386. https://doi.org/10.1038/s41586-019-1071-0.
Zumbühl, H.J., Nussbaumer, S.U., 2018. Little Ice Age glacier history of the Central and Western Alps from pictorial documents. Cuad. de Investig. Geogr. 44, 115–136. https://doi.org/10.18172/cig.3363.
Zumbühl, H.J., Steiner, D., Nussbaumer, S.U., 2008. 19th century glacier representations and fluctuations in the central and western European Alps: an interdisciplinary approach. Glob. Planet. Change, Historical and Holocene Glacier – Climate Variations 60, 42–57. https://doi.org/10.1016/j.gloplacha.2006.08.005.